

# Neurovascular Unit Model

## Documentation for Code “OO-NVU Version 1.??”

A merged NVC model of a neuron, astrocyte, smooth muscle cell,  
endothelial cell and the mechanical vessel response.

by Emiel van Disseldorp	Katharina Dormanns	Sanne van der Lelij
Joerik de Ruijter	Michelle Louise Goodman	Eva Waldhauser
Moritz Burger	Kon Zakkaroff	Tim David*

November 26, 2015

---

\*Corresponding author, Tim.david@canterbury.ac.nz

# Contents

<b>1</b>	<b>Release notes</b>	<b>3</b>
1.1	Changes to the previous version . . . . .	3
1.2	Corrections . . . . .	3
<b>2</b>	<b>Code Structure</b>	<b>4</b>
<b>3</b>	<b>Introduction</b>	<b>6</b>
3.1	Neurovascular Unit . . . . .	6
3.2	Neurovascular Coupling . . . . .	7
3.3	Mathematical Approach . . . . .	7
<b>4</b>	<b>Existing Models</b>	<b>9</b>
4.1	The Astrocyte Model . . . . .	9
4.1.1	Input Signal . . . . .	10
4.1.2	Scaling . . . . .	12
4.2	SMC and EC Model . . . . .	12
4.3	Contraction and Mechanical Model . . . . .	13
4.3.1	Contraction Model . . . . .	13
4.3.2	Mechanical Model . . . . .	14
4.4	Merging of All Models . . . . .	16
<b>5</b>	<b>Results</b>	<b>18</b>
5.1	OO-NVU 2.0 . . . . .	18
<b>6</b>	<b>Equations</b>	<b>28</b>
6.1	The Neuron and Astrocyte Model . . . . .	28
6.2	The Smooth Muscle Cell and Endothelial Cell Model . . . . .	32
6.3	The Contraction Model . . . . .	41
6.4	The Mechanical Model . . . . .	41

# 1 Release notes

## 1.1 Changes to the previous version

This is where changes should be listed.

## 1.2 Corrections

A mistake was discovered in NVU1.0 for the equation used to describe the  $K^+$  concentration in the synaptic cleft. The original equation subtracted the change in astrocytic  $K^+$  concentration from the  $K^+$  influx from the neuron. This was incorrect since not all channels lead from the astrocyte to the synaptic cleft. The BK-channel describes the flux from the astrocyte to the perivascular space, and therefore this flux was added to the equation. Fortunately, this mistake led to very small changes, and it did not significantly change the model outcomes. Figure 1 shows the old and the corrected results for the flux through the BK-channel, and it is clear that they practically overlap.

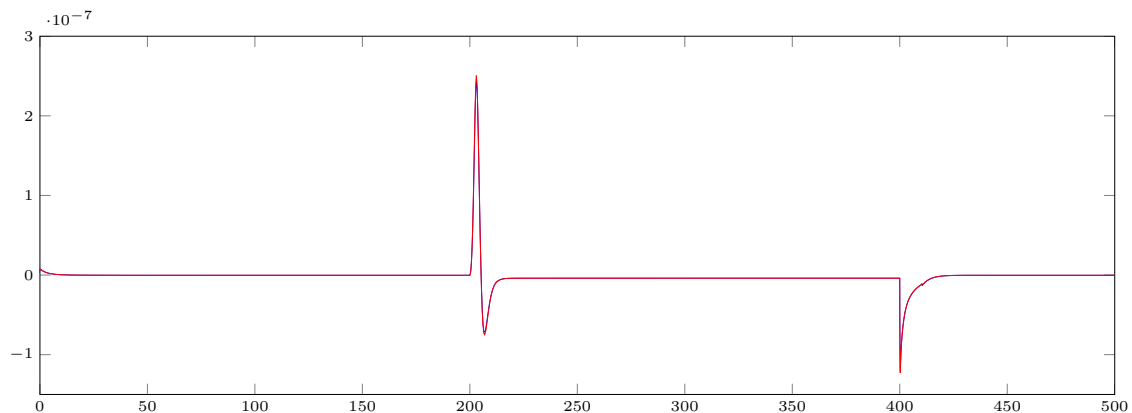


Figure 1: The flux through the BK-channel in  $\mu M$  m/s for the old (blue) and corrected (red) simulation

## 2 Code Structure

The three core classes, the `Astrocyte`, `SMCEC` and `WallMechanics`, correspond to the components of the NVU model, namely the astrocyte model, the SMC and EC model, and the mechanical contraction cell model. For a given model component, all fluxes and ODEs are grouped together in the code of the corresponding class. The `NVU` class uses the three core component classes to collect the state variable and derivatives values and pass them to the `ode15s` solver for stiff problems. All classes in OO-NVU code are subclasses of the MATLAB's `handle` class which makes them appear as reference object to avoid unnecessary object duplication on assignment. Figure 2 shows the public interfaces for all OO-NVU classes.

For a proper OO development and complexity management in the future the `Astrocyte`, `SMCEC` and the `WallMechanics` classes should have a common superclass with the shared interface (at least) and functionality. –Kon

The following features apply to the `Astrocyte`, `SMCEC` and `WallMechanics` classes:

1. The core classes rely on the class constructors to initialise the parameters with the help of the class-specific function `parse_inputs(varargin)`. The constructors also initialise the variable indices, initial conditions and the output indices.
2. In every core class the `rhs` method contains the algebraic and state variables, as well as the corresponding equations.
3. The `shared(self, ~, u)` method, where present, provides the access to the shared algebraic or state variables used as input variables in the other model components where appropriate.

The code in the file `nvu_script.m` provides a number of use-cases for running the NVU model. The code Listing 1 shows an example of setting the options for the ODE solver `ode15s` specifying the `odeopts` parameter, however the code works well with default tolerances. The `simulate()` method of the `NVU` class start the simulation.

Listing 1: Initialisation of the NVU model components.

```
1 odeopts = odeset('RelTol', 1e-03, 'AbsTol', 1e-03, 'MaxStep', 1, ...  
    'Vectorized', 1);  
2  
3 nv = NVU(Astrocyte(), ...  
4 WallMechanics(), ...  
5 SMCEC('J_PLC', 0.18), ...  
6 'odeopts', odeopts);  
7  
8 nv.simulate()
```

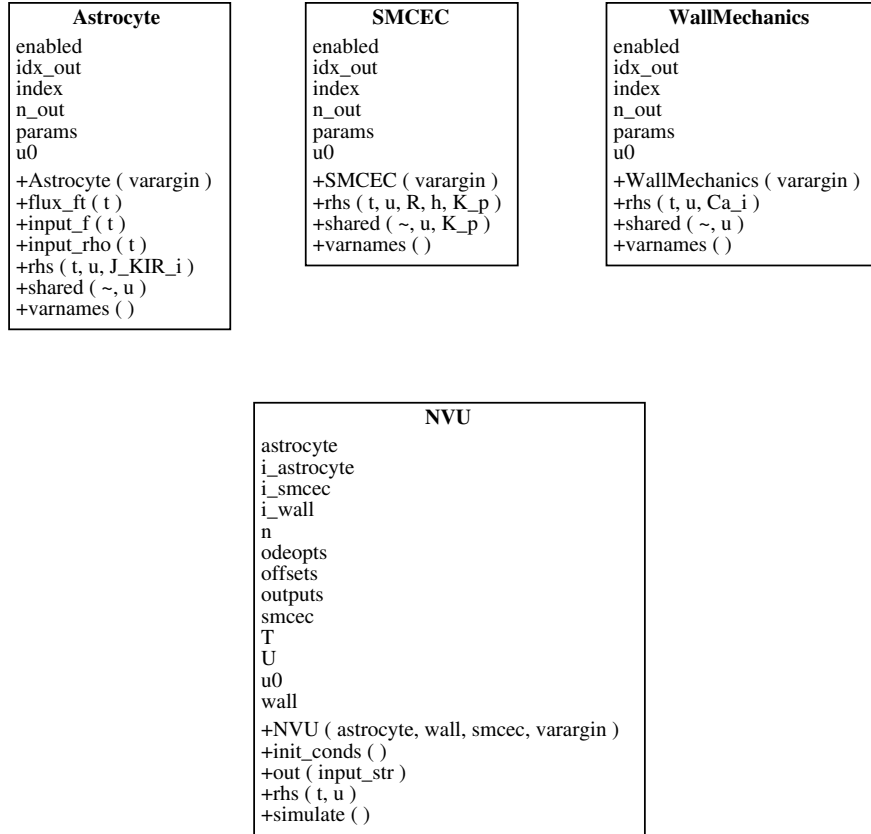


Figure 2: UML class diagram for the OO NVU code.

This is the first draft of this section. Suggestions as to what needs to be expanded further? Include more code listings? –Kon

Remove the code structure files used in the previous documentation version when this version is done. –Kon

### 3 Introduction

#### 3.1 Neurovascular Unit

The cerebral cortex, a highly complex component of the human brain and part of the grey matter (*substantia grisea*), mainly consists of neurons (NEs), unmyelinated axons and glial cells such as astrocytes (ACs). It forms the outer layer of *cerebrum* and *cerebellum* and is veined with capillary blood vessels that provide the brain tissue with glucose and oxygen (Shipp [11]). These arterioles are surrounded by endothelial cells (ECs) that form a thin layer on the interior surface of arterioles (*intima*). The outer layer of the arteriole consists of smooth muscle cells (SMCs), which are aligned in circumferential direction. They define the contractile unit of the vessel and regulate its diameter by contraction and dilation.

A neurovascular unit (NVU) defined in this research includes one cell of each of the described types and is graphically pictured in Figure 4.

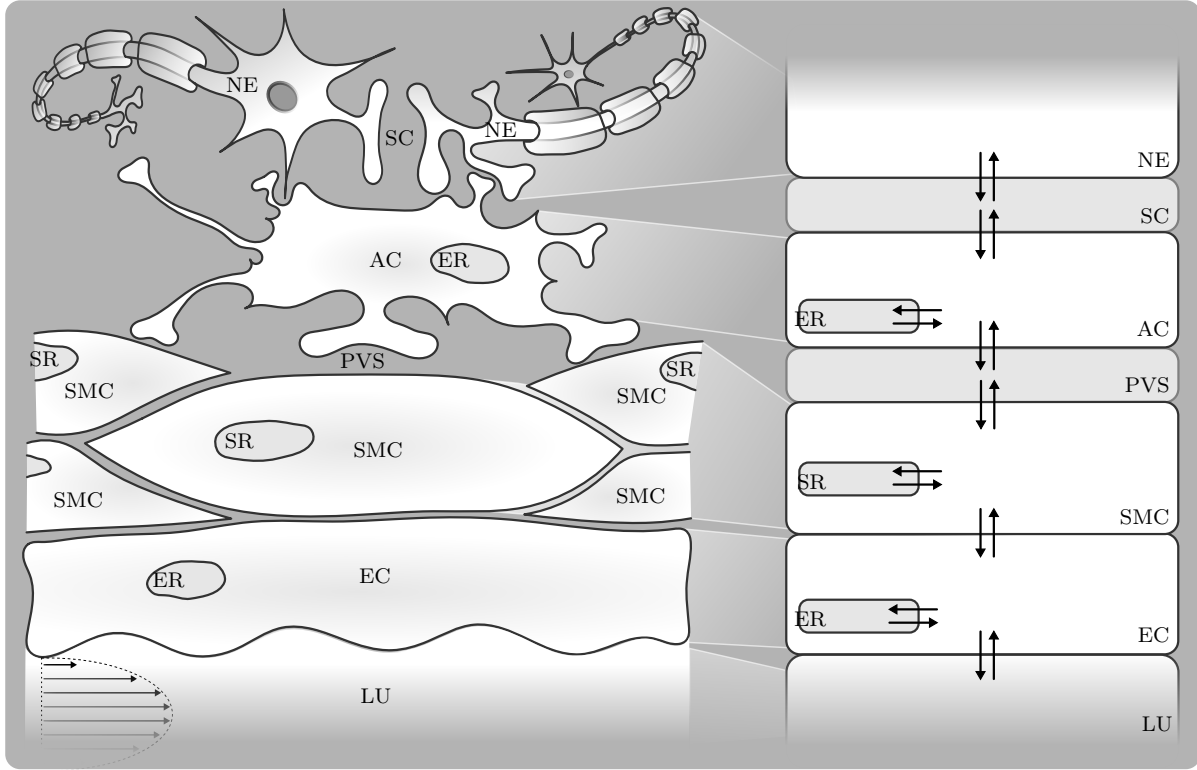


Figure 3: **Overview of different cells and domains that form a neurovascular unit.** NE - Neuron, SC - Synaptic Cleft, AC - Astrocyte, ER - Endoplasmic Reticulum, PVS - Perivascular Space, SMC - Smooth Muscle Cell, SR - Sarcoplasmic Reticulum, EC - Endothelial Cell, LU - Lumen with indicated blood flow. Intercellular communication via the exchange of ions is indicated by arrows.

Each of the cell types and the spaces in between play an important role within the process of neurovascular coupling (NVC, see Section 3.2). The synaptic cleft (SC) is the space between an axon terminal and dendrite of two different NEs in which neurotransmitters are released. It is enclosed by the star-shaped AC that can take up released neurotransmitters. Protoplasmic ACs are polarized cells which can temporarily buffer extracellular  $K^+$ , which is one of the key mechanisms within NVC. The astrocytic endoplasmatic reticulum (ER), an isolated space in the cytosol, contains  $IP_3$ -sensitive  $Ca^{2+}$  channels, which can release  $Ca^{2+}$ -ions into the cytosol. The perivascular space (PVS) is located between the end feet of an AC and the arteriole. In the PVS, ion exchange occurs between the arterial wall and the AC. The ECs form a monolayer on the luminal side of the vessel in which all cells are aligned in the direction of the flow. It prevents passive diffusion of bigger molecules, while small ones, such as  $O_2$ ,  $Ca^{2+}$  or  $IP_3$ , can pass through. It also functions as an active organ sensing wall shear stress which plays an important role in the NO-mediated pathway. Together with the SMC layer the endothelium forms the blood brain barrier (BBB), the physical frontier between brain tissue and blood vessel. SMC contraction occurs by actin and myosin filaments forming cross-bridges. The rate of contraction is dependent on the SMC cytosolic  $Ca^{2+}$  concentration.

### 3.2 Neurovascular Coupling

Neurovascular coupling (NVC), or functional hyperaemia, describes the local vasodilation and -contraction due to neuronal activation. The change in the vessel diameter (vasoreactivity) controls the blood flow and thereby the cerebral supply of oxygen and glucose.

Each cell type plays an important specific role during the process of NVC. Communication between cells is based on an exchange of ions through pumps and channels. These ion fluxes contribute to changes in cytosolic and intercellular species concentration and cell membrane potentials.

There are several pathways that can lead to vasocontraction or -dilation and are mediated by different signalling molecules, such as  $K^+$ ,  $Ca^{2+}$ , EET, NO and 20-HETE. Neurotransmitters are released by the NE into the SC and can bind to receptors on dendrites of other neurons and astrocytes. This leads to a cascade of chemical reactions and the opening and closing of ion channels which influences the fluxes and concentrations.

### 3.3 Mathematical Approach

The physiological models are based on a set of differential equations that describe the mass conservation of ions and molecules passing from one cell or domain to another. The simulations describe time-dependent ion fluxes and changes in membrane potential modelled by reaction rates that describe the kinetics which are physiologically validated by experimental data from the literature. This approach assumes homogeneous behaviour of a variable in a certain subdomain i.e. the spatial gradient of a variable in every subdomain is negligible.

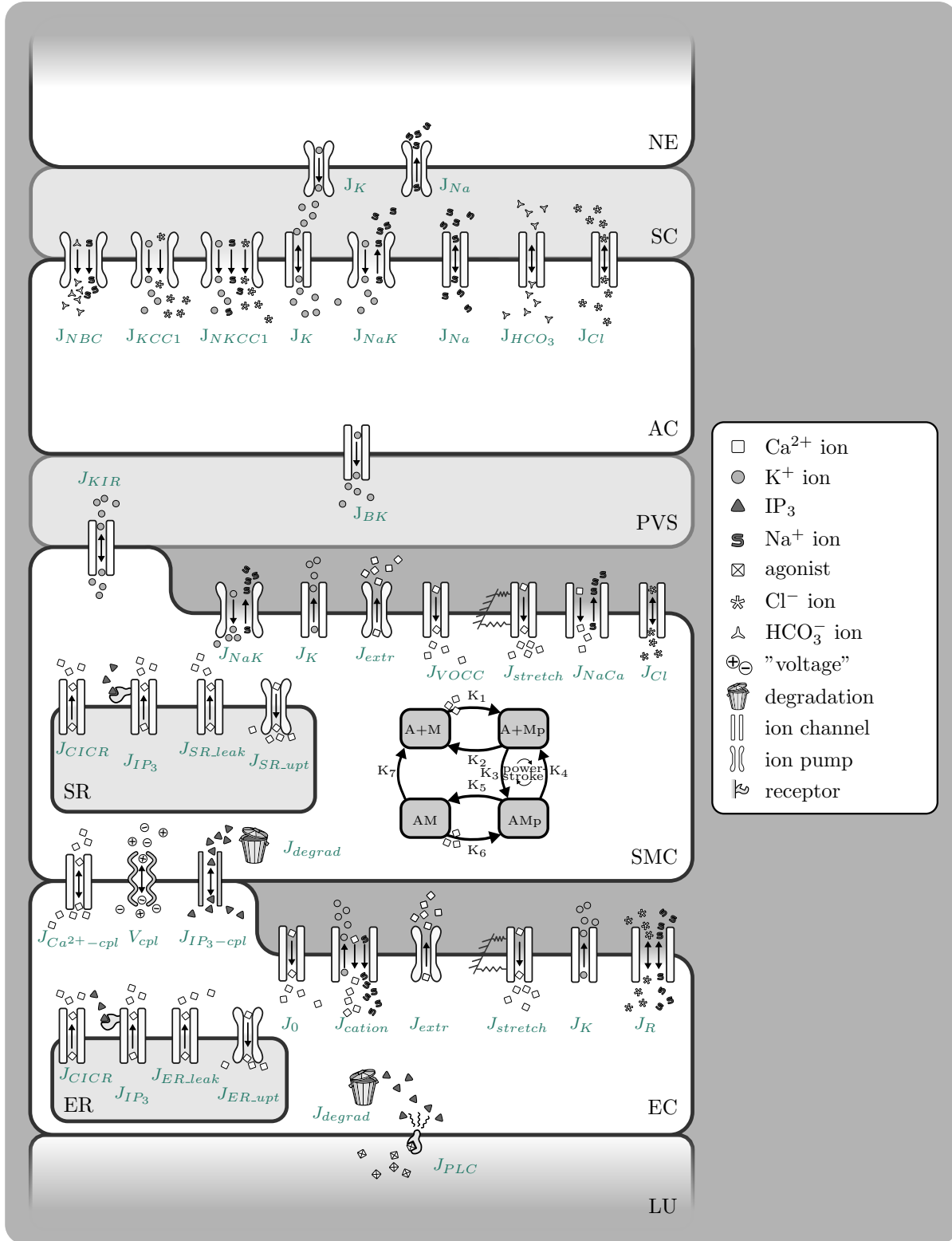


Figure 4: **Overview of model.** NE - Neuron, SC - Synaptic Cleft, AC - Astrocyte, ER - Endoplasmic Reticulum, PVS - Perivascular Space, SMC - Smooth Muscle Cell, SR - Sarcoplasmic Reticulum, EC - Endothelial Cell, LU - Lumen.



## 4 Existing Models

The present mathematical model is the first of its kind, leading the way in modelling the whole neurovascular coupling process. Starting with the neuronal activation we build up to the response in vessel diameter, utilizing all cell types and crucial pathways. It is based on three existing models.

- **The Astrocyte Model** - describes the crucial biochemical processes within the astrocyte (AC, Østby et al. [10], reviewed by Donk and Kock [1]).
- **The SMC and EC Model** - describes the behaviour and the main ion fluxes within the smooth muscle cell (SMC) and endothelium cell (EC). This model is based on that of Koenigsberger et al. [7].
- **The Contraction and Mechanical Model** - describes the relationship between the cytosolic calcium ( $\text{Ca}^{2+}$ ) concentration in the SMC and the contraction and dilation of the SMC by a myosin phosphorylation and cross-bridge based on the models of Hai and Murphy [6] and Kelvin Voigt.

### 4.1 The Astrocyte Model

During neural activity,  $\text{K}^+$  is released into the synaptic cleft (SC) by active neurons (NEs). In the astrocyte model, this is implemented by an influx of  $\text{K}^+$  ( $J_{K_s}$ ) with a corresponding  $\text{Na}^+$  uptake by the neuron ( $J_{Na_s}$ , Figure 5). The increase of  $\text{K}^+$  in the SC results in an increased  $\text{K}^+$  uptake by the AC which consequently undergoes depolarization. This results in a  $\text{K}^+$  efflux from distant portions of the cell. Since most of the  $\text{K}^+$  conductance of ACs is located at the end-feet, the outward current-carrying  $\text{K}^+$  would flow out of the cell largely through these locations. Consequently, the  $\text{K}^+$  is 'siphoned' to the end-feet of the astrocyte and released into the perivascular space (PVS) which leads to an increase of  $\text{K}^+$  in the PVS. This  $\text{K}^+$  release leads to a repolarization of the membrane voltage and is the input signal for the second (SMC & EC) part of this model.

The AC model contains different types of active and passive ion channels. These ion channels and pumps are captured in a set of differential equations to describe the conservation of mass for the corresponding species concentrations in the SC, the AC and the PVS. The ion channels for potassium ( $J_{KCC1}$ ,  $J_{NKCC1}$ ,  $J_K$ ,  $J_{NaK}$  and  $J_{BK}$ ), sodium ( $J_{NBC}$ ,  $J_{NKCC1}$ ,  $J_{NaK}$  and  $J_{Na}$ ), chloride ( $J_{KCC1}$ ,  $J_{NKCC1}$  and  $J_{Cl}$ ) and bicarbonate ( $J_{HCO_3}$ ) are included. Note that the bicarbonate and chlorine fluxes are coupled with the  $\text{Na}^+$  and  $\text{K}^+$  fluxes to obtain a neutral in- or efflux membrane voltage-wise.

The release of glutamate from the neuron in the synaptic cleft is simulated by creating a smooth pulse function  $\rho$  that describes the ratio of bound to total glutamate receptors on the synapse end of the astrocyte. This induces an  $IP_3$  release into the cell, causing the release

of Calcium from the ER into the cytosol, which then leads to the production of EET. The  $K^+$  release into the PVS is controlled by the BK-channels. The opening of the BK-channels is regulated by the membrane voltage, as well as the EET and  $Ca^{2+}$  concentration.

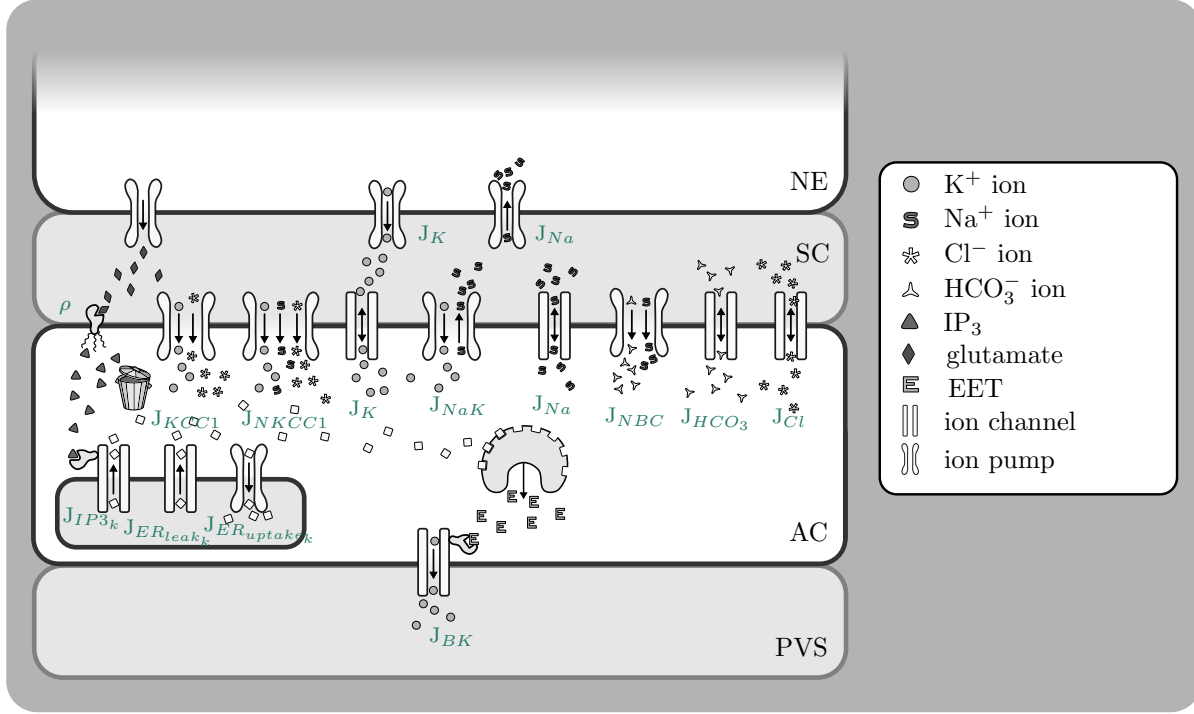


Figure 5: **Illustration of the astrocyte model.** All modelled fluxes are pictured, note that the indices (k - Astrocyte (AC), s - Synaptic Cleft (SC), p - Perivascular Space (PVS)) are left out for clarity reasons.

#### 4.1.1 Input Signal

In this model, a neuronal excitation was mimicked by an efflux of  $K^+$  into the synaptic cleft (SC) and a simultaneous equal influx of  $Na^+$  into the neuron from the SC (Østby et al. [10], see equations in section 6.1). The time-dependent input signal ( $f(t)$ , see figure 6) starts at  $t = 200s$  and ends at  $t = 210s$ . To estimate the profile  $f(t)$  of the  $K^+$  efflux/ $Na^+$  influx, it is assumed that the  $K^+$  efflux has a shape of a beta distribution with the governing parameters  $\alpha$  and  $\beta$  such that the profile is optimized according to two criteria [10]:

1. The time from the start until the attaining maximum level of the  $K^+$  concentration in the SC is 5s.
2. The level of the  $K^+$  concentration in the SC at  $t = 30s$  is 60% of the minimal level.

These two criteria take into account that  $\beta$  is set at a value of  $\beta = 5$ .

In order to enhance the maximum  $K^+$  level in the SC to reach the order of magnitude proposed by Filosa et al. [2], the amplitude of the input signal  $f(t)$  is scaled up by the value  $F_{input}$ . The quantity of  $K^+$  ions pumped into the AC can be derived by taking the integral of the flux  $k_c f(t)$  over time, where  $k_c$  is a constant that relates the input signal  $f(t)$  to the  $K^+$  influx.

The amount of released ions are slowly buffered back by the neuron after the input signal terminates. This is modelled by a decay constant within the time interval  $230s \leq t \leq 240s$ . The integral of this block function is the same as the integral of the beta distribution in order to return to the baseline.

Beside this neuronal input signal, the NKCC1 and KCC1 co-transporters are only enabled when the neuronal ion release and spatial buffering are applied. With both parameters added, the behaviour is modelled by a block function with the value  $-F_{input}$  with a default value of zero (Figure 6).

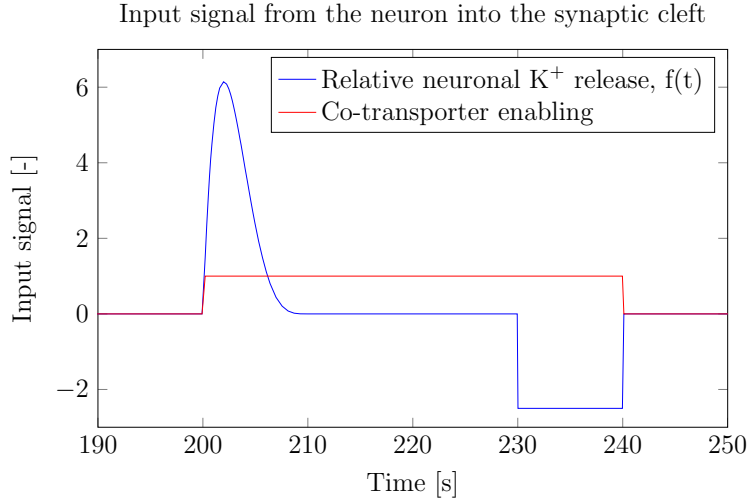


Figure 6: **The input signals used in the astrocyte model.** The  $K^+$  efflux modelled by a beta distribution and buffered back afterwards (blue). The NKCC1 and KCC1 co-transporters are enabled when the neuronal ion release and spatial buffering is applied, modelled by a block function (red).

### 4.1.2 Scaling

The flux equations used in the AC model are based on the model of Østby et al. [10]. Their intention was to look at the volume changes of the AC and SC, therefore the volumes of both are variables in this model and all fluxes are scaled by a volume-surface ratio ( $R_k$  and  $R_s$ , see Equations 6 and 7, respectively). It is assumed that the sum of the volumes of the AC and SC is a constant ( $R_{tot}$ ). Due to osmotic pressure, the volume changes. We could show that the changes are comparatively small in our model and it would be justifiable to leave out the scaling factors. However, at the moment they are included because the given fluxes of Østby et al. [10] are scaled by the volume-surface ratio. It should be considered in future versions to eliminate the scaling factors by multiplying the fluxes with an adequate constant.

## 4.2 SMC and EC Model

The SMC and EC model is based on the work of Koenigsberger et al. [7], see Figure 7. This model is extended by adding an inward-rectifier potassium (KIR) channel in the SMC ( $J_{KIR}$ , [2]) in order to create a connection between the Astrocyte model and the SMC and EC model.

The input signal for this model is the  $K^+$  concentration in the PVS which is increased by the efflux of astrocytic potassium after neuronal activity.

The raise in  $K^+$  in the PVS activates the KIR channel on the SMC, causing them to open extruding more potassium into the PVS. This efflux of  $K^+$  hyperpolarizes the SMC membrane and causing the voltage-operated  $Ca^{2+}$  channels to close, preventing the influx of  $Ca^{2+}$  into the SMC cytosol.

The cytosolic  $Ca^{2+}$  concentrations in the SMC and EC and that in the sarcoplasmic reticulum (SR) and endoplasmic reticulum (ER), respectively, are described by a set of differential equations. In- and effluxes of  $K^+$  are given by the following ion channel and pumps:  $J_{KIR}$ ,  $J_{NaK}$  and  $J_K$ .  $Ca^{2+}$  leaves the SR via the channels:  $J_{CICR}$ ,  $J_{IP_3}$  and  $J_{SR,leak}$  and enters it by  $J_{SR,upt}$ . The in- and efflux of  $Ca^{2+}$  are modelled with  $J_{extr}$ ,  $J_{VOCC}$ ,  $J_{stretch}$  and  $J_{NaCa}$ . Note that these fluxes link the cytosol with the extracellular matrix. Here again, a chloride pump is included,  $J_{Cl}$ , to return to the resting membrane potential.

Physiologically, ECs and SMCs are connected by gap junctions that allow an intercellular exchange of molecules and voltage. Koenigsberger et al. [7] include the coupling factors  $J_{Ca^{2+}-cpl}^{EC-SMC}$ ,  $V_{cpl}^{EC-SMC}$  and  $J_{IP_3-cpl}^{EC-SMC}$  for  $Ca^{2+}$ , voltage and  $IP_3$  coupling, respectively. The strength of the coupling can be changed in the code with the variable *CASE*.

Inositol triphosphate ( $IP_3$ ) is an important messenger molecule. It's production, in the endothelium, is triggered by agonist binding onto membrane receptors.  $IP_3$  mediates the  $J_{IP_3}$  channel, situated between the reticulum and cytosol. The production rate of  $IP_3$  is a constant over time and can be changed by altering the variable  $J_{PLC}$  within the mathematical model.

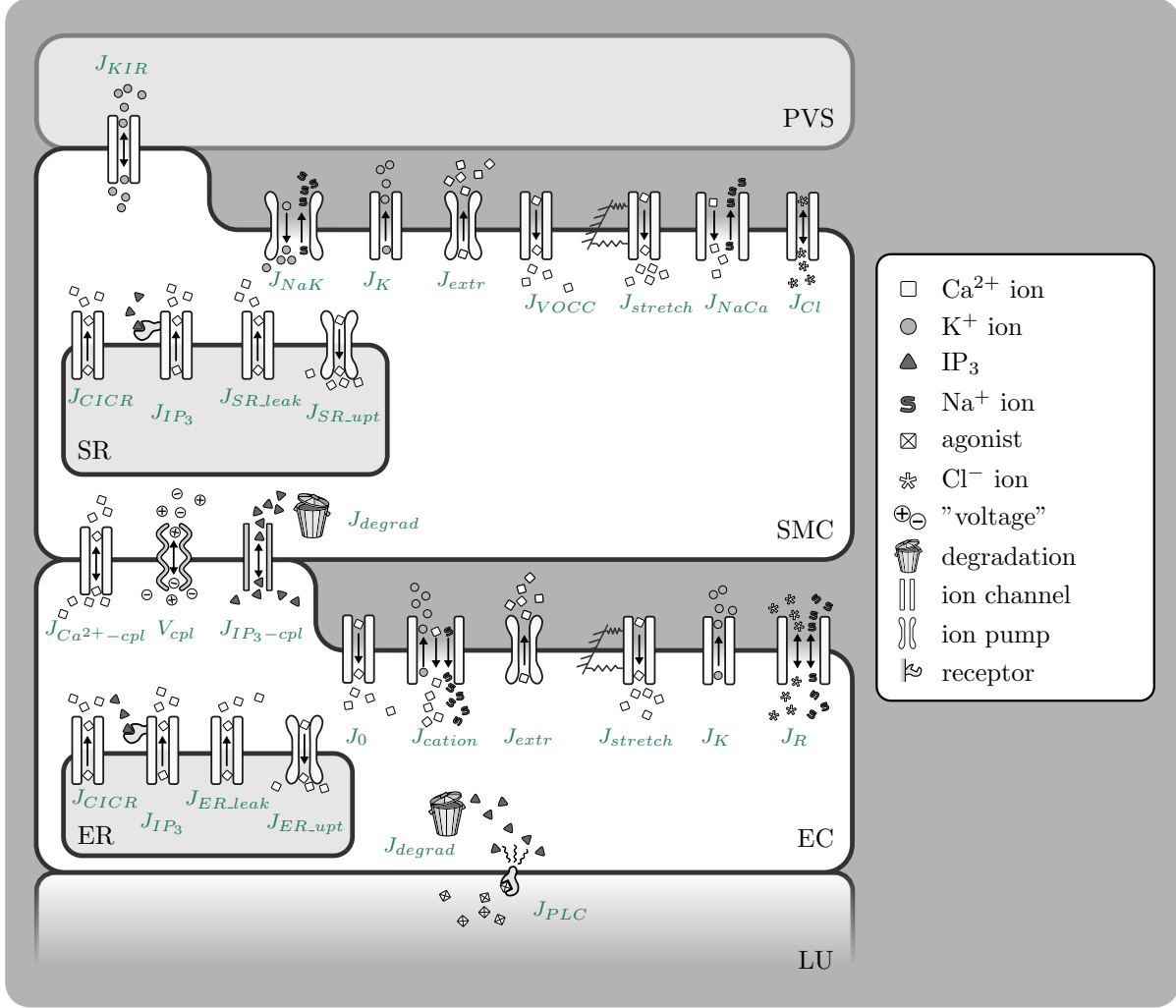


Figure 7: **Illustration of the SMC and EC model.** All modelled fluxes are pictured, note that the indices (k - Astrocyte (AC), s - Synaptic Cleft (SC), p - Perivascular Space (PVS)) are left out for clarity reasons.

Note that the model of Koenigsberger et al. [7] already includes  $\text{Ca}^{2+}$ -buffering in the SMC and EC.

## 4.3 Contraction and Mechanical Model

### 4.3.1 Contraction Model

The contraction and mechanical part of the model is based on the model of Hai and Murphy [6], which describes the formation of cross bridges between the myosin and actin filaments (Figure 8). This is coupled with a Kelvin-Voigt model that is used to describe the visco-

elastic behaviour of the arterial wall (Figure 9).

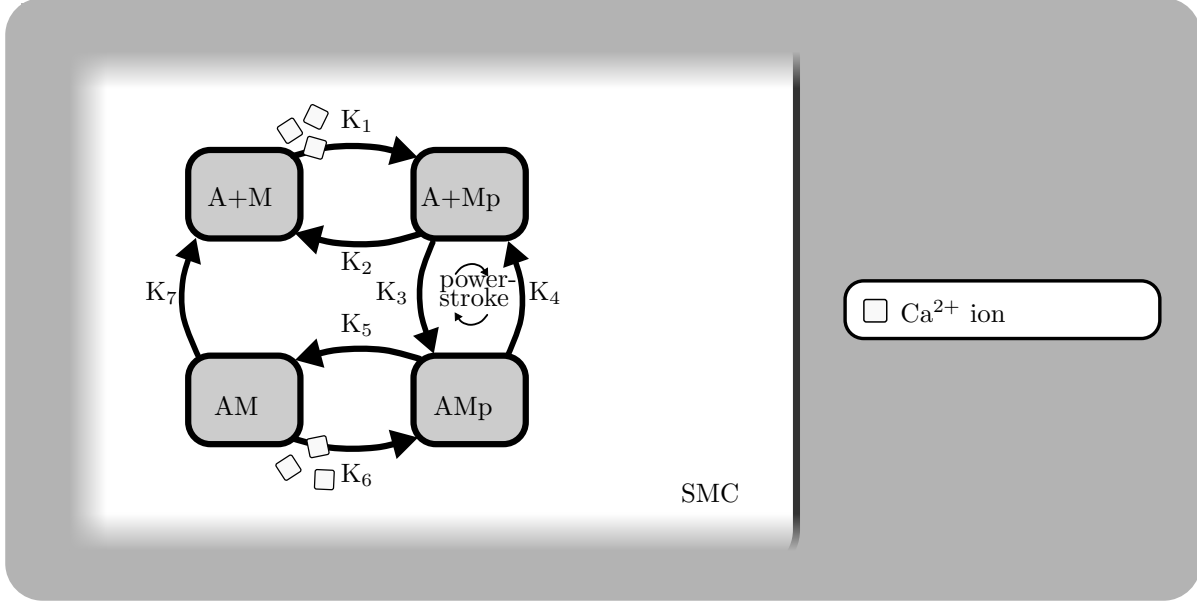


Figure 8: **Illustration of the contraction model within the smooth muscle cell.**

The  $Ca^{2+}$  concentration in the SMC is the input signal for the cross bridge model of Hai and Murphy [6]. The model uses four possible states for the formation of myosin: free nonphosphorylated cross bridges (M), free phosphorylated cross bridges (Mp), attached phosphorylated cross bridges (AMp) and attached dephosphorylated latch bridges (AM). The dynamics of the fraction of myosin in a particular state is given by four differential equations.

The active stress of the SMC is directly proportional to the fraction of attached cross bridges (AM and AMp). Using this model the relation between the cytosolic  $Ca^{2+}$  concentration and the active stress of the SMC can be derived.

#### 4.3.2 Mechanical Model

The fraction of attached myosin cross bridges is the input signal for the visco-elastic mechanical model (Kelvin Voigt, Figure 9) which describes the changes in radius over time. The pressure inside the vessel wall is taken as a constant and the circumferential stress is calculated using the Laplacian law.

The Young's modulus and initial radius of the vessel wall is divided into an active and a passive part and is a function of the attached myosin cross-bridges. The active and passive Young's modulus are based and fitted on experimental data of [?] which is shown in Figure 10.

Figure 10 shows that the initial radius ( $R_0$ ) decreases when the fraction of attached myosin cross bridges ( $F$ ) are increased (the intersection with the x-axis). The figure also

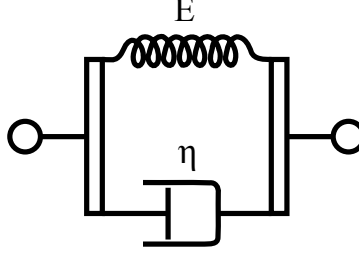


Figure 9: Schematic overview of a Kelvin Voigt model.

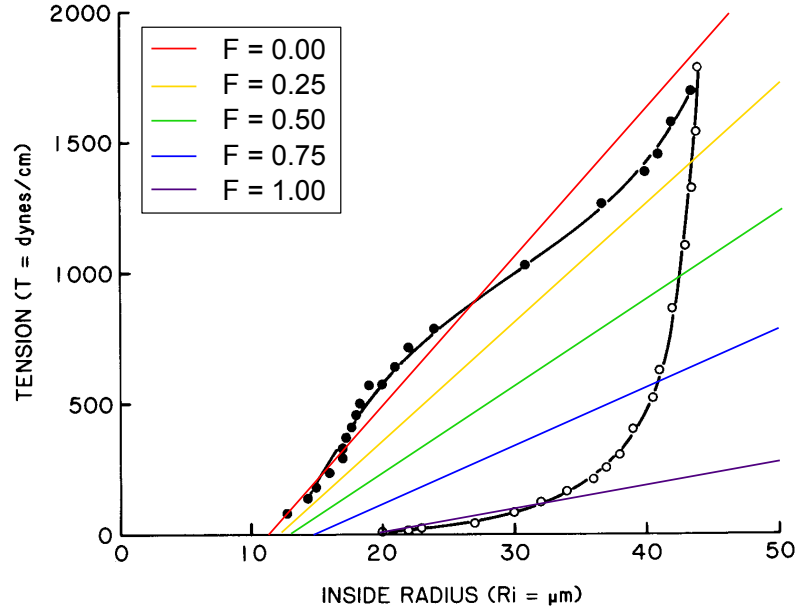


Figure 10: Linearisation for the Young's modulus and initial radius on the data of [?] for different values of  $F$ .

shows that the Young's modulus, represented by the slope of the lines in the tension-strain graph, increases when  $F$  increases. The linearisations of the Young's modulus can be described by:

$$T = \frac{\Delta T}{\Delta R}(R - R_0) , \quad (1)$$

where  $T$  is the tension of the vessel and  $\frac{\Delta T}{\Delta R}$  is the slope of the linearisations in Figure 10.

## 4.4 Merging of All Models

The Astrocyte model and the SMC and EC model are linked by the SC and the PVS. The  $K^+$  input signal of the neuron is pumped into the SC and taken up afterwards by the AC. The most important ion pumps and channels in this process are the  $K^+$  channels in the neuron which releases the  $K^+$  input, the  $Na^+/K^+$  pump and  $K^+$  channel in the AC which pump the released  $K^+$  into the AC. The result of this is an efflux of  $K^+$  at the end feet of the astrocyte using the BK-channel. Consequently, the membrane voltage of the astrocyte re-polarizes and the  $K^+$  concentration in the PVS increases. This increased  $K^+$  concentration activates the KIR channel in the SMC and start to pump out more  $K^+$  from the SMC into the PVS. The increased efflux of  $K^+$  hyperpolarises the SMC membrane voltage and as a result of that the VOCC closes and prevents the influx of  $Ca^{2+}$  into the SMC. Summarising, the neuronal input signal leads to a decrease of  $Ca^{2+}$  influx by the VOCC channels and therefore a decrease of the intracellular  $Ca^{2+}$  concentration. This leads to a decreased fraction of attached myosin bridges in the Hai and Murphy [6] model, resulting in vessel dilation in the visco-elastic mechanical model. An overview of the whole model is shown in Figure 11.



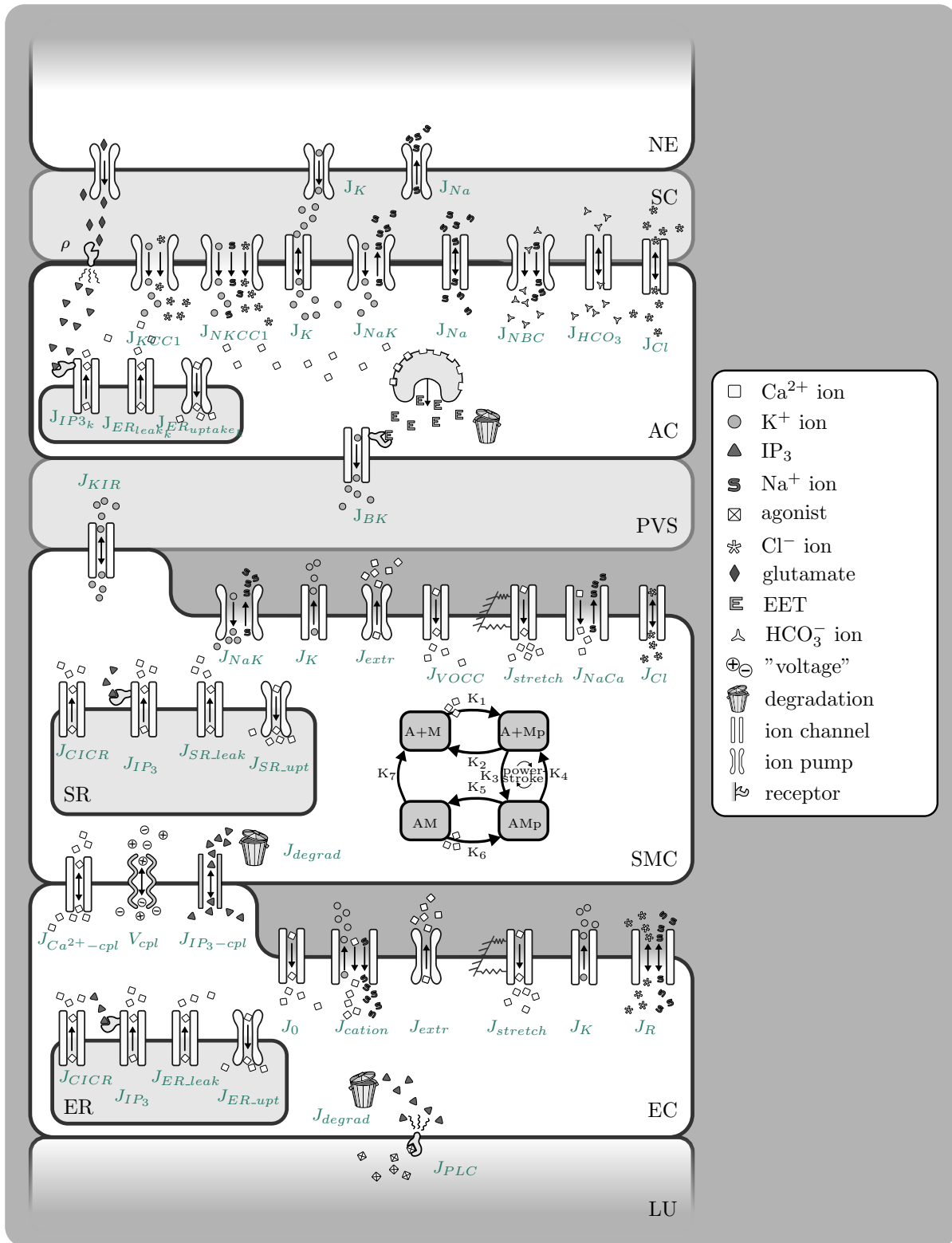


Figure 11: All Models.

## 5 Results

### 5.1 OO-NVU 2.0

#### Potassium input signal (figure 12)

At the top the neuronal  $K^+$  input signal is shown. This input signal is pumped into the SC by the NE. As a result of that, there is more  $K^+$  taken up by the AC in the beginning of the input pulse, and released at the end of the input pulse. In the second graph the membrane potential of the AC is shown over time. When the  $K^+$  concentration in the SC is increased the membrane voltage depolarises and when the  $K^+$  concentration in the SC decreases the membrane potential repolarises again. In the third graph the fluxes into the PVS are shown. In blue the flux by the astrocytic BK channel, and in green the flux by the KIR channel in the SMC is shown. The drop in the middle of the KIR flux is caused because the SMC becomes in a oscillatory state and therefore the efflux by the KIR channel follows the  $Ca^{2+}$  waves inside the SMC. The bottom figure shows the  $K^+$  concentration in the PVS.

#### Neurovascular Coupling Overview (figure 13)

This figure describes the main pathway from the synaptic cleft to the radius change. It starts with a  $K^+$  concentration in the synaptic cleft, followed by the flux trough the BK-channel determined in the astrocyte, leading to an increased  $K^+$  concentration in the perivascular space. This causes an increased  $K^+$  influx trough the KIR channel, changing the membrane voltage of the SMC. The  $Ca^{2+}$  flux through the VOCC increases, decreasing the  $Ca^{2+}$  concentration in the SMC and thereby inducing vasodilation.

#### AC State Variables (figure 14)

The graphs display the concentrations of  $K^+$ ,  $Ca^{2+}$ , Cl and  $HCO_3$  in the astrocyte and  $K^+$  in the SC and PVS. These concentrations, together with the membrane voltage contribute to the opening of the BK-channel in their own way. The open state of the BK channel determines the potassium flux from the astrocyte to the perivascular space, where it induces vascular contraction.

#### AC Fluxes (figure 15)

All ion fluxes that enter or leave the astrocyte.

#### SMC EC State Variables and Coupling (figure 16)

The graphs in this figure shows the solutions of the differential equations of the SMC and EC, including the intracellular  $Ca^{2+}$  concentration, the  $IP_3$  concentration, the sarcoplasmic (SMC) or endoplasmic (EC)  $Ca^{2+}$  concentration, the membrane voltage and the coupling fluxes between EC and SMC.

### **SMC Fluxes (figure 17)**

In these figures the coupling and the fluxes in the SMC are shown. When one of the fluxes is negative, it means that the direction of the flux is in the opposite than it is defined in the equations. These figures show that when the neuronal signal is given, the VOCC closes and that the SMC contracts.

### **EC Fluxes (figure 18)**

All ion fluxes that enter or leave the EC.

### **Contraction Model and Radius (figure 19)**

In this figure the fraction of the four states (M, Mp, AMp, AM) of myosin in the SMC are shown at the top. At the bottom left the fraction of attached cross bridged myosin (the sum of AM and AMp) is shown. And at the bottom right the radius is plotted over time. The increase in vessel diameter is in the expected order of magnitude.

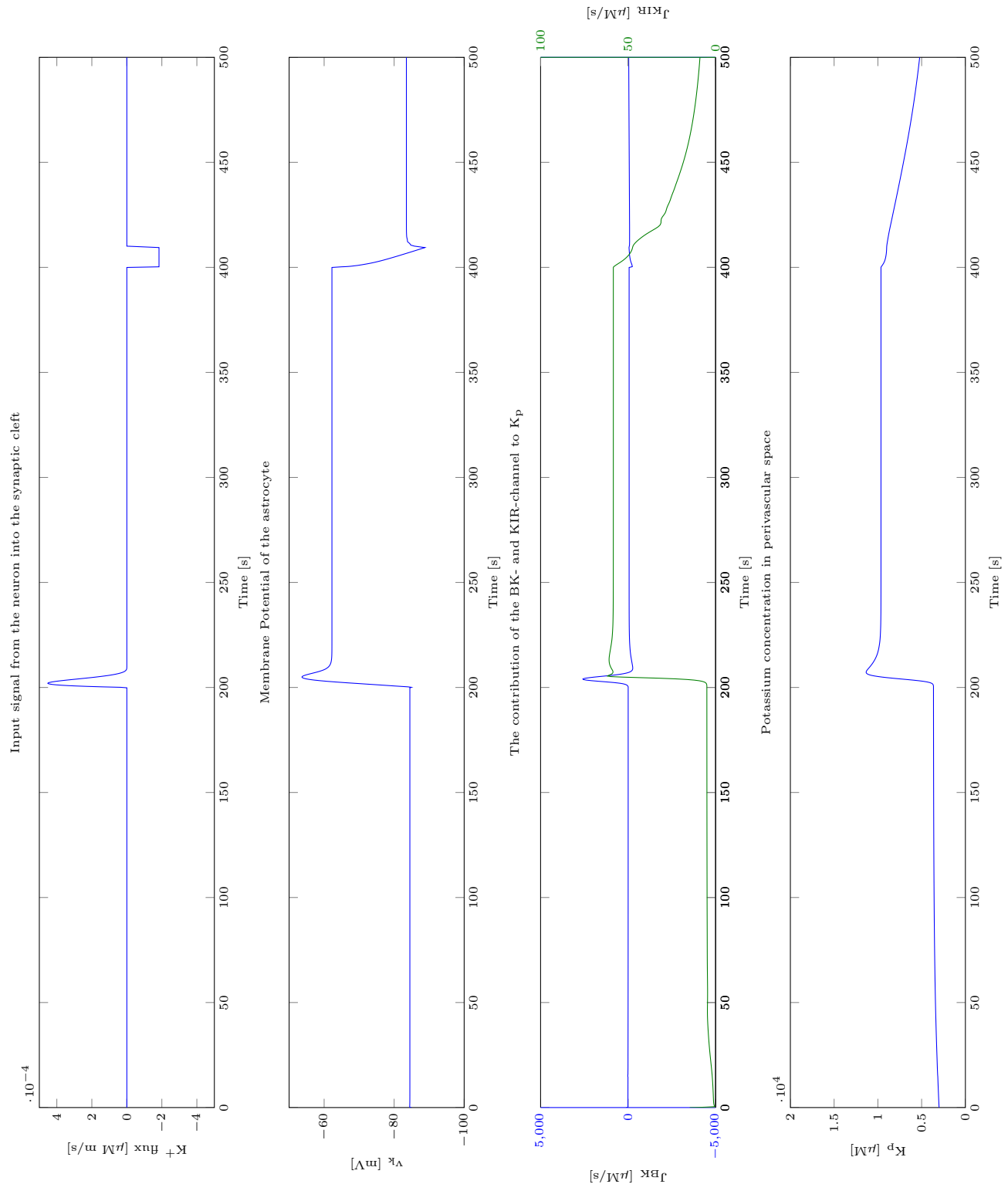


Figure 12: The input signal.

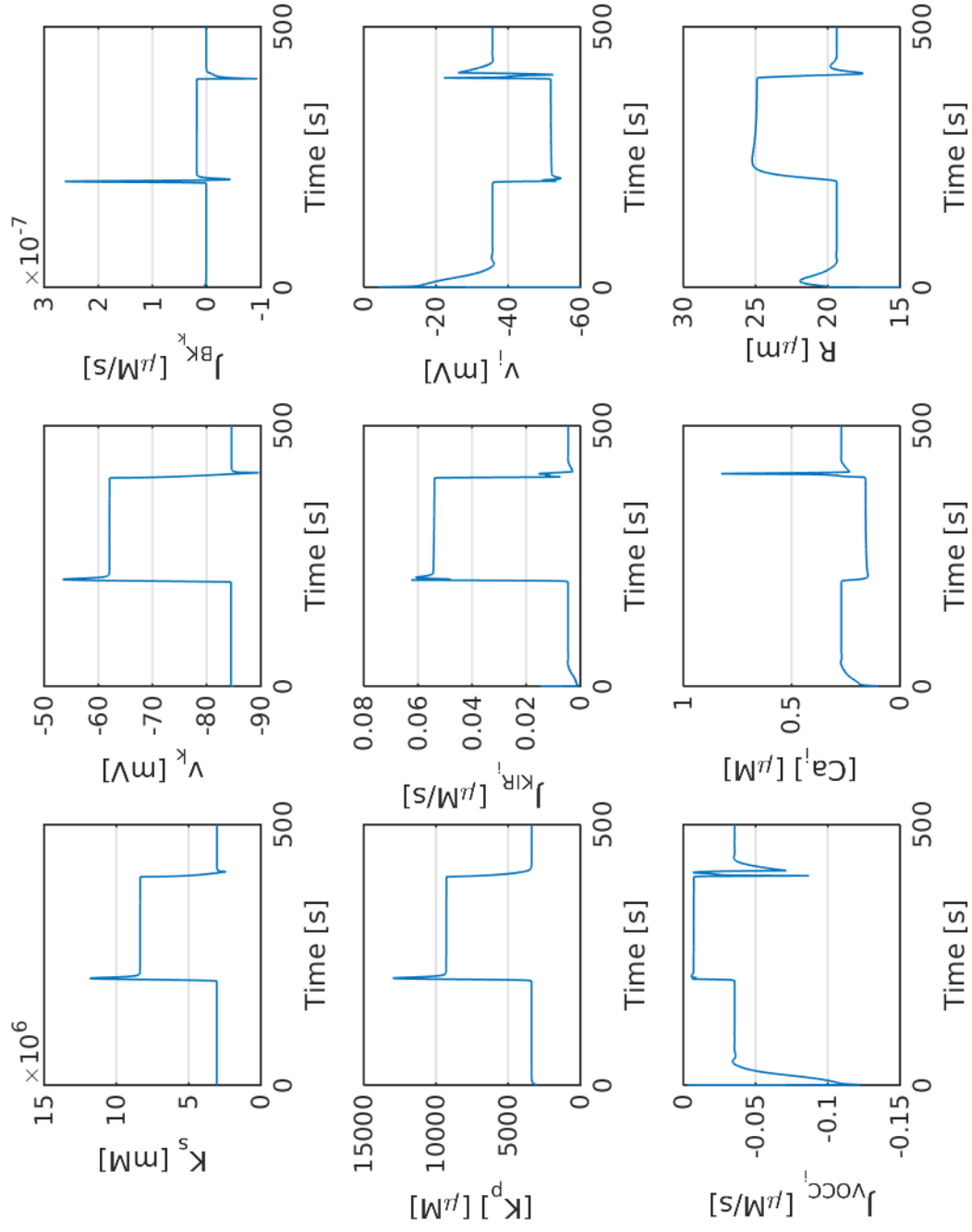


Figure 13: Neurovascular Coupling Overview.

AC State Variables.png

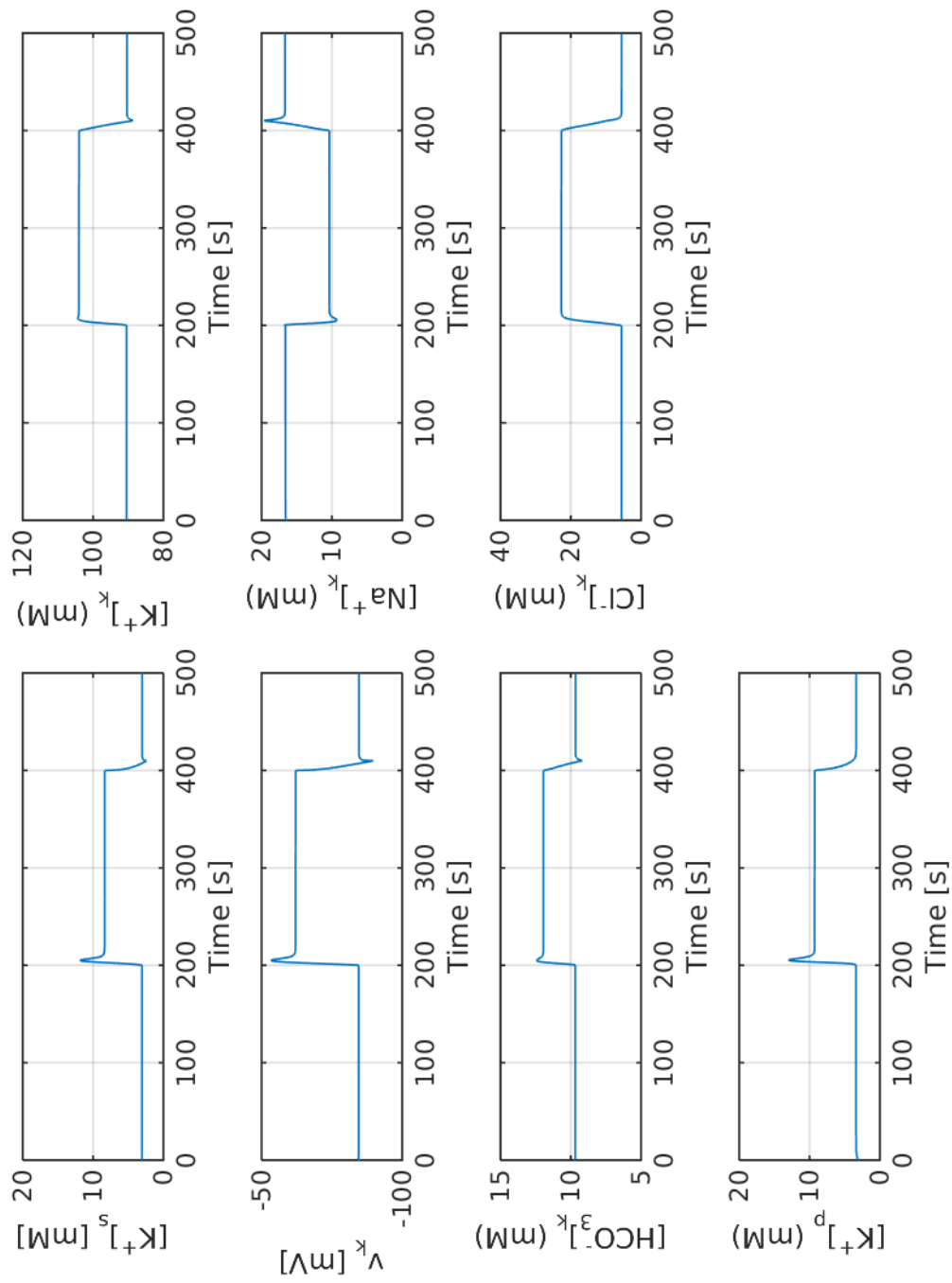


Figure 14: AC State Variables.

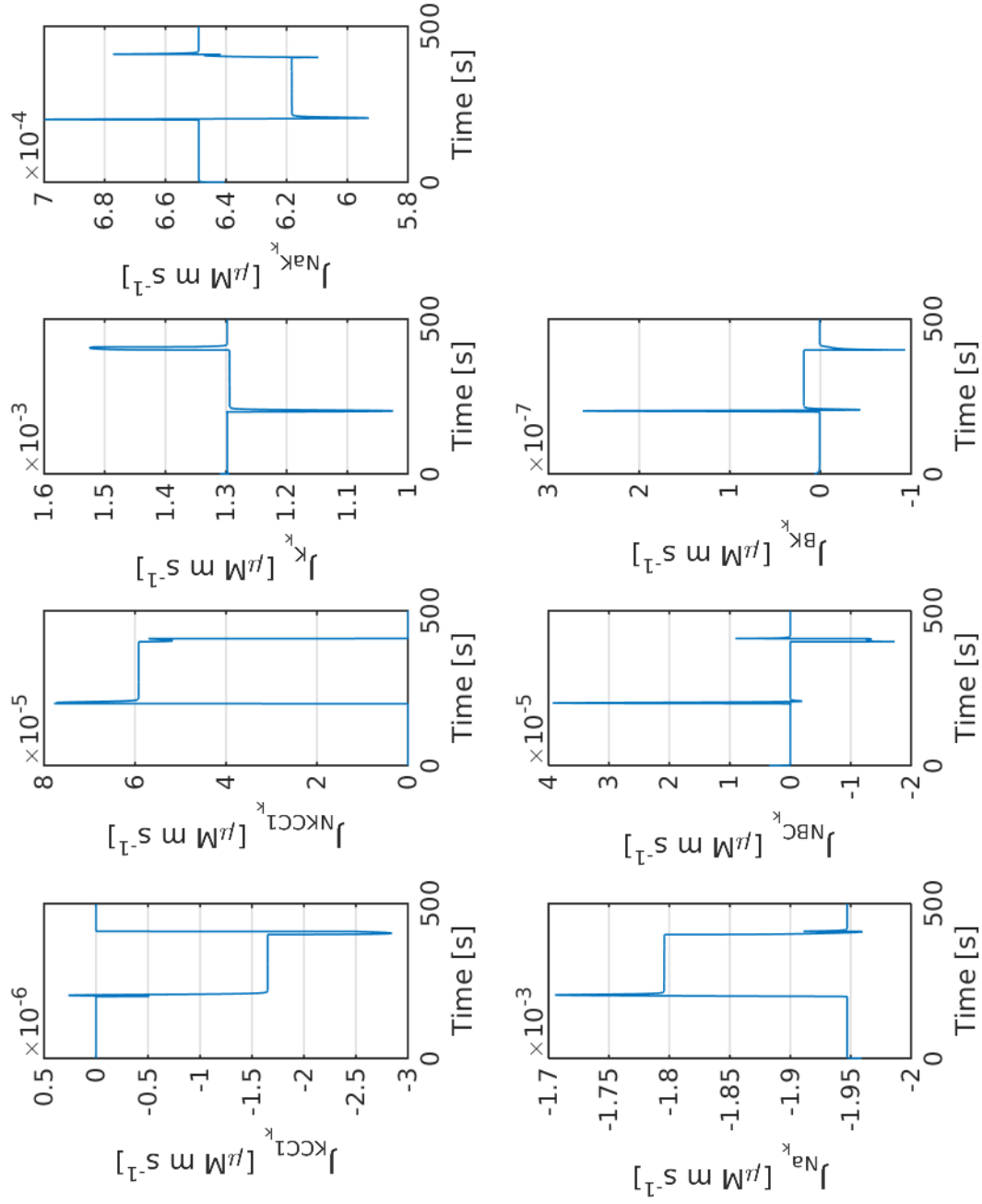


Figure 15: AC Fluxes.

SMC EC State Variables and Coupling.png

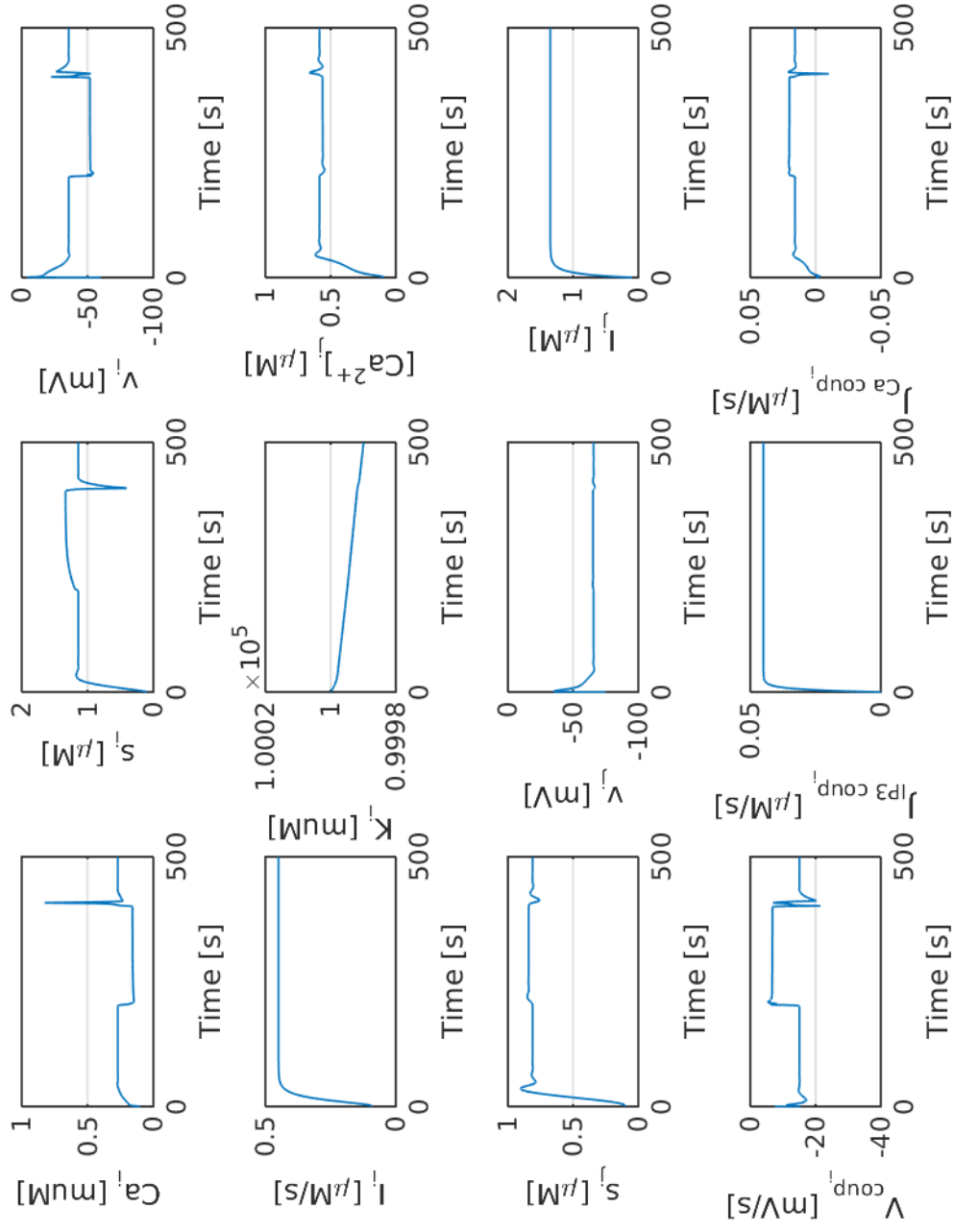


Figure 16: SMC EC State Variables and Coupling.



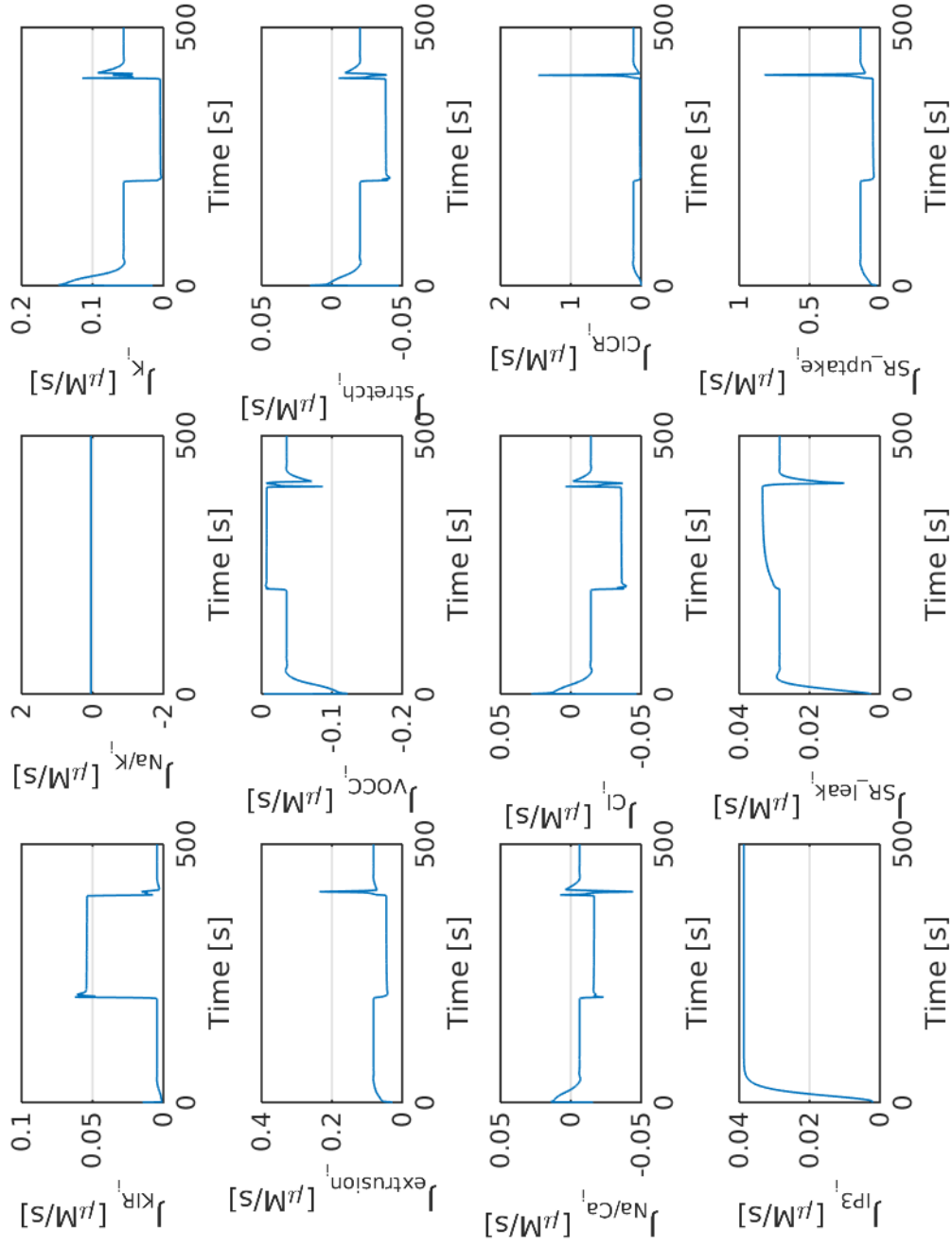


Figure 17: SMC Fluxes.

EC Fluxes.png

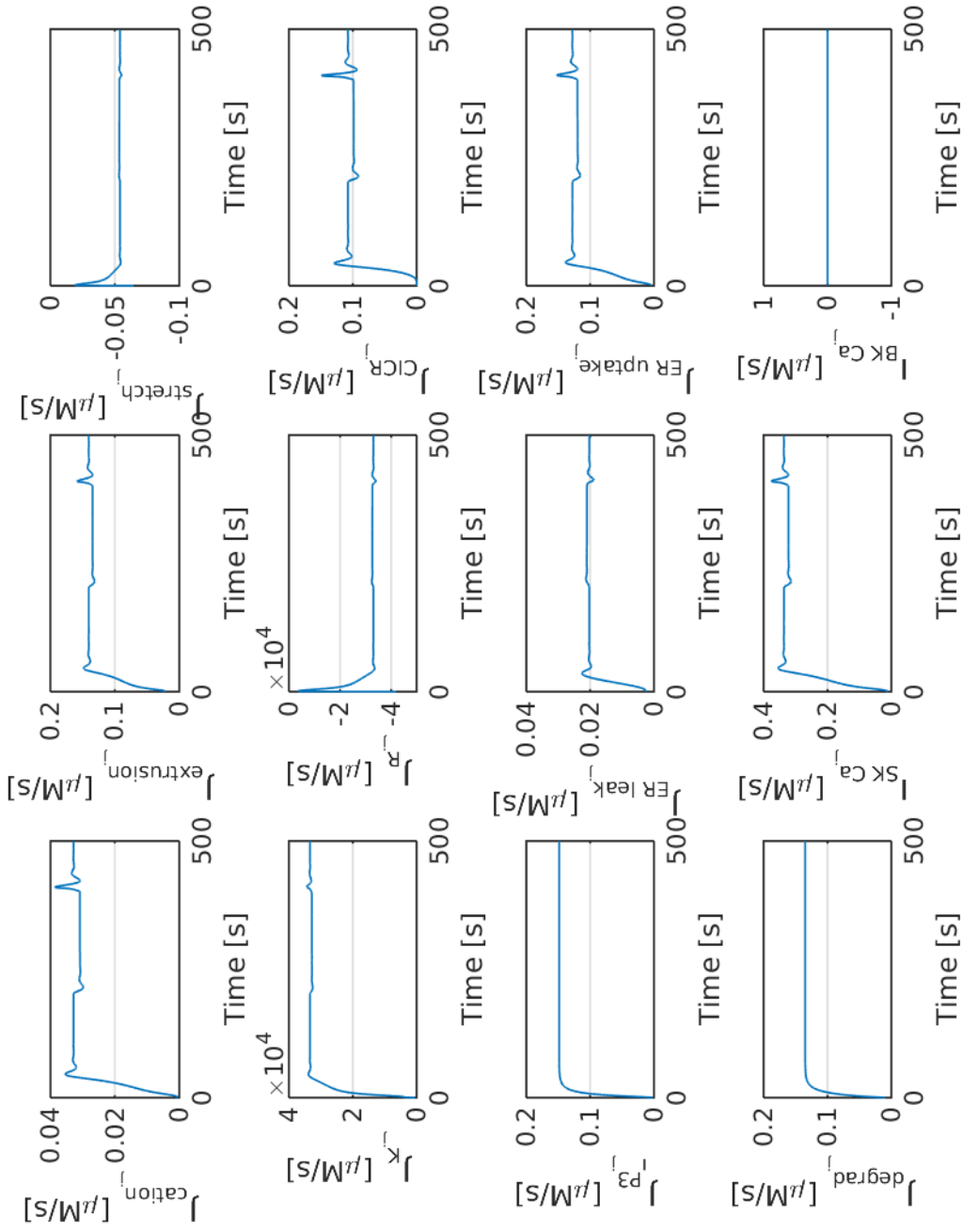


Figure 18: EC Fluxes.

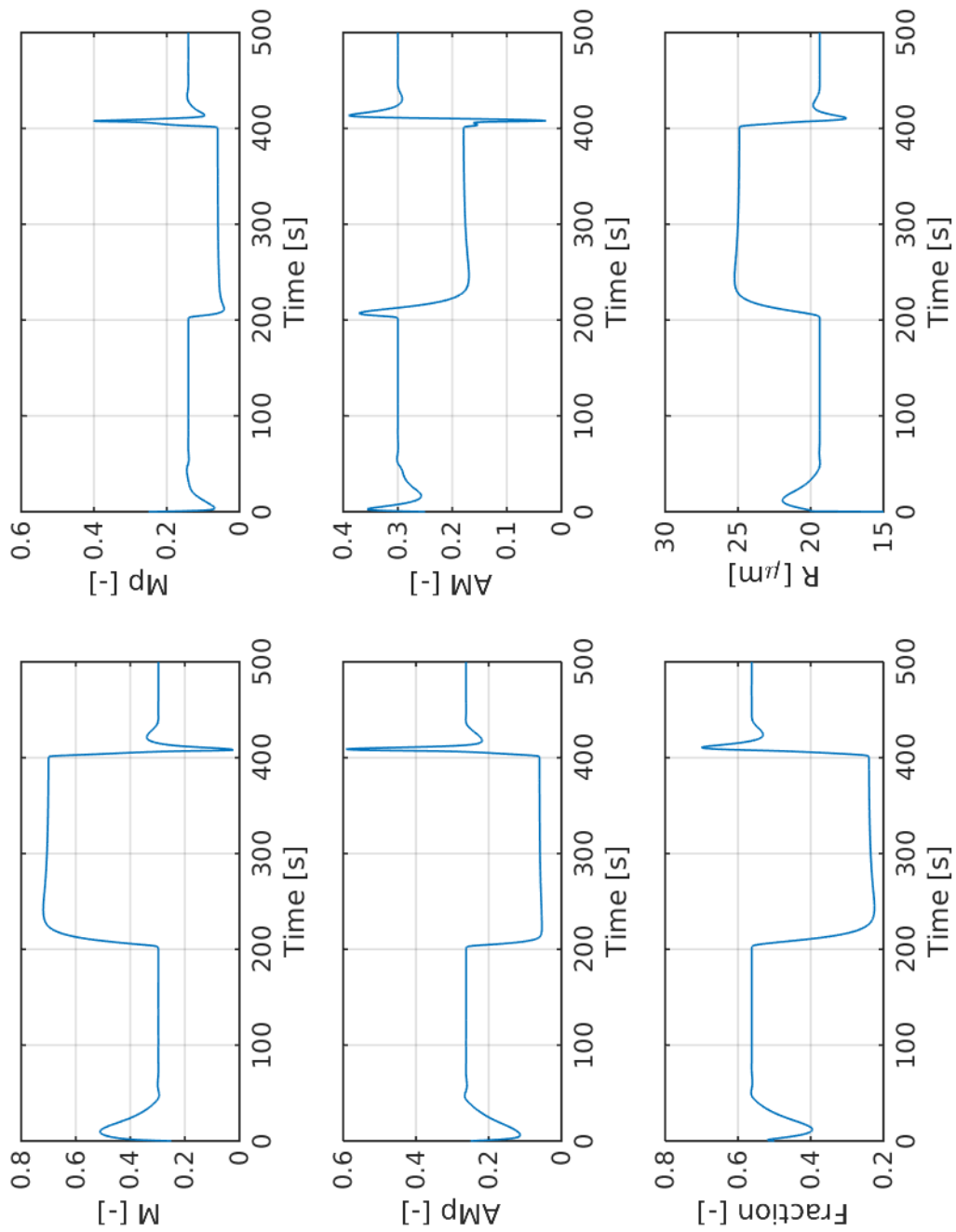


Figure 19: Contraction Model and Radius.

## 6 Equations

Some units need to be corrected in this documentation!

### 6.1 The Neuron and Astrocyte Model

#### Input signals

Neuronal  $K^+$  input signal (dim.less):

$$f_{K/Na}(t) = \begin{cases} F_{\text{input}} \frac{(\alpha_n + \beta_n - 1)!}{(\alpha_n - 1)!(\beta_n - 1)!} \left( \frac{1 - (t - t_0)}{\Delta t_2} \right)^{\beta_n - 1} \left( \frac{t - t_0}{\Delta t_2} \right)^{\alpha_n - 1}, & \text{for } t_0 \leq t < t_1 \\ -F_{\text{input}}, & \text{for } t_2 \leq t \leq t_3 \\ 0, & \text{otherwise} \end{cases} \quad (2)$$

End of neuronal pulse (s):

$$t_1 = t_0 + \Delta t \quad (3)$$

Start of back-buffering (s):

$$t_2 = t_0 + \Delta t_1 \quad (4)$$

End of back buffering (s):

$$t_3 = t_1 + \Delta t_1 \quad (5)$$

$F_{\text{input}}$	amplitude scaling factor	2.5	ME <sup>1</sup>
$\alpha_n$	beta distribution constant	2	ME
$\beta_n$	beta distribution constant	5	ME
$t_0$	start of neuronal activation	400 s	ME
$\Delta t_1$	length of neuronal activation	200 s	ME
$\Delta t_2$	time-scaling factor	10 s	[10]

1

#### Scaling

AC volume-area ratio (in m):

$$\frac{dR_k}{dt} = L_p([Na^+]_k + [K^+]_k + [Cl^-]_k + [HCO_3^-]_k - [Na^+]_s - [K^+]_s - [Cl^-]_s - [HCO_3^-]_s + \frac{X_k}{R_k}) \quad (6)$$

SC volume-surface ratio (in m):

$$R_s = R_{\text{tot}} - R_k \quad (7)$$

<sup>1</sup>Model Estimation

<sup>2</sup>corrected value/unit obtained from **CellML**

<sup>3</sup>corrected value/unit obtained from communication with author

$L_p$	total water permeability per unit area of the astrocyte	$2.1 \times 10^{-9} \text{ m } \mu\text{M}^{-1} \text{ s}^{-1}$	[10] <sup>2</sup>
$X_k$	Number of negatively charged impermeable ions trapped within the astrocyte divided by the astrocyte membrane area	$12.41 \times 10^{-3} \text{ } \mu\text{M m}$	[10]
$R_{\text{tot}}$	Total volume surface ratio AC + SC $((V_{sc} + V_k)/A_k)$	$8.79 \times 10^{-8} \text{ m}$	[10] <sup>2</sup>
$A_k$	characteristic exchange surface area	$3.7 \times 10^{-9} \text{ m}^2$	[10] <sup>3</sup>

## Conservation Equations

### Synaptic Cleft

$\text{K}^+$  concentration in the SC (times the SC volume-area ratio  $R_s$ ; in  $\mu\text{M m}$ ):

$$\frac{dN_{\text{K},s}}{dt} = k_C f(t) - \frac{dN_{\text{K},k}}{dt} - J_{\text{BK},k}; \quad [\text{K}^+]_s = \frac{N_{\text{K},s}}{R_s} \quad (8)$$

$\text{Na}^+$  concentration in the SC (times the SC volume-area ratio  $R_s$ ; in  $\mu\text{M m}$ ):

$$\frac{dN_{\text{Na},s}}{dt} = -k_C f(t) - \frac{dN_{\text{Na},k}}{dt}; \quad [\text{Na}^+]_s = \frac{N_{\text{Na},s}}{R_s} \quad (9)$$

$\text{HCO}_3^-$  concentration in the SC (times the SC volume-area ratio  $R_s$ ; in  $\mu\text{M m}$ ):

$$\frac{dN_{\text{HCO}_3,s}}{dt} = -\frac{dN_{\text{HCO}_3,k}}{dt}; \quad [\text{HCO}_3^-]_s = \frac{N_{\text{HCO}_3,s}}{R_s} \quad (10)$$

$k_C$	Input scaling parameter	$7.35 \times 10^{-5} \text{ } \mu\text{M m s}^{-1}$	[10]
-------	-------------------------	---	------

### Astrocyte

$\text{K}^+$  concentration in the AC (times the AC volume-area ratio  $R_k$ ; in  $\mu\text{M m}$ ):

$$\frac{dN_{\text{K},k}}{dt} = -J_{\text{K},k} + 2J_{\text{NaK},k} + J_{\text{NKCC1}_k} + J_{\text{KCC1}_k} - J_{\text{BK},k}; \quad [\text{K}^+]_k = \frac{N_{\text{K},k}}{R_k} \quad (11)$$

$\text{Na}^+$  concentration in the AC (times the AC volume-area ratio  $R_k$ ; in  $\mu\text{M m}$ ):

$$\frac{dN_{\text{Na},k}}{dt} = -J_{\text{Na},k} - 3J_{\text{NaK},k} + J_{\text{NKCC1}_k} + J_{\text{NBC},k}; \quad [\text{Na}^+]_k = \frac{N_{\text{Na},k}}{R_k} \quad (12)$$

$\text{HCO}_3^-$  concentration in the AC (times the AC volume-area ratio  $R_k$ ; in  $\mu\text{M m}$ ):

$$\frac{dN_{\text{HCO}_3,k}}{dt} = 2J_{\text{NBC},k}; \quad [\text{HCO}_3^-]_k = \frac{N_{\text{HCO}_3,k}}{R_k} \quad (13)$$

$\text{Cl}^-$  concentration in the AC (times the AC volume-area ratio  $R_k$ ; in  $\mu\text{M m}$ ):

$$\frac{dN_{\text{Cl},k}}{dt} = \frac{dN_{\text{Na},k}}{dt} + \frac{dN_{\text{K},k}}{dt} - \frac{dN_{\text{HCO}_3,k}}{dt}; \quad [\text{Cl}^-]_k = \frac{N_{\text{Cl},k}}{R_k} \quad (14)$$

Open probability of the BK channel (non-dim.):

$$\frac{dw_k}{dt} = \phi_w (w_\infty - w_k) \quad (15)$$

## Perivascular Space

K<sup>+</sup> concentration in the PVS (in  $\mu\text{M}$ ):

$$\frac{dK_p}{dt} = \frac{J_{\text{BK},k}}{R_k R_{pk}} + \frac{J_{\text{KIR},i}}{R_{ps}} - R_{\text{decay}}([K^+]_p - [K^+]_{p,\min}); \quad (16)$$

$R_{pk}$	Volume ratio of PVS to AC	$10^{-3}$ [-]	[9]
$R_{ps}$	Volume ratio of PVS to SMC	$10^{-3}$ [-]	[9]
$R_{\text{decay}}$	Decay rate	$0.05 \text{ s}^{-1}$	M.E.
$[K^+]_{p,\min}$	min K <sup>+</sup> concentration	$3 \times 10^3 \text{ }\mu\text{M}$	M.E.

## Fluxes

K<sup>+</sup> flux (times the AC volume-area ratio  $R_k$ ; in  $\mu\text{M m s}^{-1}$ ):

$$J_{\text{K},k} = \frac{g_{K,k}}{F}(v_k - E_{\text{K},k}) \quad (17)$$

Na<sup>+</sup> flux (times the AC volume-area ratio  $R_k$ ; in  $\mu\text{M m s}^{-1}$ ):

$$J_{\text{Na},k} = \frac{g_{\text{Na},k}}{F}(v_k - E_{\text{Na},k}) \quad (18)$$

Na<sup>+</sup> and HCO<sub>3</sub> flux through the NBC channel (times the AC volume-area ratio  $R_k$ ; in  $\mu\text{M m s}^{-1}$ ):

$$J_{\text{NBC},k} = \frac{g_{\text{NBC},k}}{F}(v_k - E_{\text{NBC},k}) \quad (19)$$

Cl and K<sup>+</sup> flux through the KCC1 channel (times the AC volume-area ratio  $R_k$ ; in  $\mu\text{M m s}^{-1}$ ):

$$J_{\text{KCC1},k} = C_{\text{input}} \frac{g_{\text{KCC1},k}}{F} \frac{R_{\text{gas}} T}{F} \ln \left( \frac{[K^+]_s [Cl^-]_s}{K_k [Cl^-]_k} \right) \quad (20)$$

Na<sup>+</sup>, K<sup>+</sup> and Cl flux through the NKCC1 channel (times the AC volume-area ratio  $R_k$ ; in  $\mu\text{M m s}^{-1}$ ):

$$J_{\text{NKCC1},k} = C_{\text{input}} \frac{g_{\text{NKCC1},k}}{F} \frac{R_{\text{gas}} T}{F} \ln \left( \frac{Na_s [K^+]_s [Cl^-]_s^2}{Na_k K_k [Cl^-]_k^2} \right) \quad (21)$$

Flux through the sodium potassium pump (times the AC volume-area ratio  $R_k$ ; in  $\mu\text{M m s}^{-1}$ ):

$$J_{\text{NaK},k} = J_{\text{NaK},\max} \frac{Na_k^{1.5}}{Na_k^{1.5} + K_{\text{Na},k}^{1.5}} \frac{[K^+]_s}{[K^+]_s + K_{\text{K},s}} \quad (22)$$

K<sup>+</sup> flux through the BK channel (times the AC volume-area ratio  $R_k$ ; in  $\mu\text{M m s}^{-1}$ ):

$$J_{\text{BK},k} = \frac{g_{\text{BK},k}}{F} w_k (v_k - E_{\text{BK},k}) \quad (23)$$

$F$	Faraday's constant	$9.649 \times 10^4 \text{ C mol}^{-1}$	
$R_{\text{gas}}$	Gas constant	$8.315 \text{ J mol}^{-1} \text{ K}^{-1}$	
$T$	Temperature	300 K	
$g_{K,k}$	Specific ion conductance of potassium	$40 \times 10^3 \text{ } \Omega^{-1} \text{ m}^{-2}$	[10]
$g_{\text{Na},k}$	Specific ion conductance of sodium	$1.314 \times 10^3 \text{ } \Omega^{-1} \text{ m}^{-2}$	[10]
$g_{\text{NBC},k}$	Specific ion conductance of the NBC cotransporter	$7.57 \times 10^2 \text{ } \Omega^{-1} \text{ m}^{-2}$	[10]
$g_{\text{KCC1},k}$	Specific ion conductance of the KCC1 cotransporter	$10 \text{ } \Omega^{-1} \text{ m}^{-2}$	[10]
$g_{\text{NKCC1},k}$	Specific ion conductance of the NKCC1 cotransporter	$55.4 \text{ } \Omega^{-1} \text{ m}^{-2}$	[10]
$J_{\text{NaK},\text{max}}$	Maximum flux through the NaKATPase pump	$1.42 \times 10^{-3} \text{ } \mu\text{M m s}^{-1}$	[10]
$G_{\text{BK},k}$	Potassium conductance of the BK channel	$4.3 \times 10^3 \text{ pS}$	[4]
$C_{\text{input}}$	Block function to switch the channel on and off	0 ; 1 [-]	
$K_{\text{Na},k}$	Michaelis-Menten constant	$10^4 \text{ } \mu\text{M}$	
$K_{\text{K},s}$	Michaelis-Menten constant	$1.5 \times 10^3 \text{ } \mu\text{M}$	
$C_{\text{unit}}$	Unit converting factor	$10^3$	M.E.

Specific ion conductance of the BK channel ( $\Omega^{-1} \text{ m}^{-2}$ ):

$$g_{\text{BK},k} = \frac{G_{\text{BK},k} \times 10^{-12}}{A_k} = 1.16 \times 10^3 \text{ } \Omega^{-1} \text{ m}^{-2} \quad (24)$$

## Additional Equations

### Synaptic Cleft

Cl concentration (times the SC volume-area ratio  $R_s$ ; in  $\mu\text{M m}$ ):

$$N_{\text{Cl},s} = N_{\text{Na},s} + N_{\text{K},s} - N_{\text{HCO}_3,s} ; \quad [\text{Cl}^-]_s = \frac{N_{\text{Cl},s}}{R_s} \quad (25)$$

### Astrocyte

Membrane voltage of the AC (V):

$$v_k = \frac{g_{\text{Na},k} E_{\text{Na},k} + g_{\text{K},k} E_{\text{K},k} + g_{\text{Cl},k} E_{\text{Cl},k} + g_{\text{NBC},k} E_{\text{NBC},k} + g_{\text{BK},k} w_k E_{\text{BK},k} - J_{\text{NaK},k} F C_{\text{unit}}}{g_{\text{Na},k} + g_{\text{K},k} + g_{\text{Cl},k} + g_{\text{NBC},k} + g_{\text{BK},k} w_k} \quad (26)$$

Nernst potential for the potassium channel (in mV):

$$E_{\text{K},k} = \frac{R_{\text{gas}} T}{z_K F} \ln \left( \frac{[\text{K}^+]_s}{[\text{K}^+]_k} \right) \quad (27)$$

Nernst potential for the sodium channel (in mV):

$$E_{\text{Na},k} = \frac{R_{\text{gas}} T}{z_{\text{Na}} F} \ln \left( \frac{Na_s}{Na_k} \right) \quad (28)$$

Nernst potential for the chloride channel (in mV):

$$E_{Cl,k} = \frac{R_{gas}T}{z_{Cl}F} \ln \left( \frac{[Cl^-]_s}{[Cl^-]_k} \right) \quad (29)$$

Nernst potential for the NBC channel (in mV):

$$E_{NBC,k} = \frac{R_{gas}T}{z_{NBC}F} \ln \left( \frac{Na_s HCO_{3,s}^2}{Na_k HCO_{3,k}^2} \right) \quad (30)$$

Nernst potential for the BK channel (in mV):

$$E_{BK,k} = \frac{R_{gas}T}{z_K F} \ln \left( \frac{[K^+]_p}{[K^+]_k} \right) \quad (31)$$

Equilibrium state BK-channel (-):

$$w_\infty = 0.5 \left( 1 + \tanh \left( \frac{v_k + v_6}{v_4} \right) \right) \quad (32)$$

Time constant associated with the opening of BK channels (in  $s^{-1}$ ):

$$\phi_w = \psi_w \cosh \left( \frac{v_k + v_6}{2v_4} \right) \quad (33)$$

$g_{Cl,k}$	Specific ion conductance of chloride	$0.879 \Omega^{-1}m^{-2}$	[10]
$z_K$	Valence of a potassium ion	1	
$z_{Na}$	Valence of a sodium ion	1	
$z_{Cl}$	Valence of a chloride ion	-1	
$z_{NBC}$	Effective valence of the NBC cotransporter complex	-1	
$v_6$	Voltage associated with the opening of half the population	22 mV or V???	[4]
$v_4$	A measure of the spread of the distribution of the open probability of the BK channel	14.5 mV or V???	[4]
$\psi_w$	A characteristic time for the open probability of the BK channel	$2.664 s^{-1}$	[4]

## 6.2 The Smooth Muscle Cell and Endothelial Cell Model

### Conservation Equations

#### Smooth muscle cell

Cytosolic  $[Ca^{2+}]$  in the SMC (in  $\mu M$ ):

$$\begin{aligned} \frac{d[Ca^{2+}]_i}{dt} = & J_{IP_3,i} - J_{upt,i} + J_{CICR_i} - J_{extr,i} + J_{leak,i} \dots \\ & - J_{VOCC,i} + J_{Na/Ca,i} + 0.1 J_{stretch,i} + J_{Ca^{2+}-coupling_i}^{SMC-EC} \end{aligned} \quad (34)$$



$[\text{Ca}^{2+}]$  in the SR of the SMC (in  $\mu\text{M}$ ):

$$\frac{d[\widehat{\text{Ca}^{2+}}]_i}{dt} = J_{\text{upt},i} - J_{\text{CICR}_i} - J_{\text{leak},i} \quad (35)$$

Membrane potential of the SMC (in mV):

$$\begin{aligned} \frac{dv_i}{dt} = \gamma_i & (-J_{\text{Na/K},i} - J_{\text{Cl},i} - 2J_{\text{VOCC},i} - J_{\text{Na/Ca},i} - J_{\text{K},i} \dots \\ & - J_{\text{stretch},i} - J_{\text{KIR},i}) + V_{\text{coupling}_i}^{\text{SMC-EC}} \end{aligned} \quad (36)$$

Open state probability of calcium-activated potassium channels (dim.less):

$$\frac{dw_i}{dt} = \lambda_i (K_{\text{act}_i} - w_i) \quad (37)$$

$\text{IP}_3$  concentration on the SMC (in  $\mu\text{M}$ ):

$$\frac{d[\text{IP}_3]_i}{dt} = J_{\text{IP}_3\text{-coupling}_i}^{\text{SMC-EC}} - J_{\text{degr},i} \quad (38)$$

$\text{K}^+$  concentration in the SMC (in  $\mu\text{M}$ ):

$$\frac{d[\text{K}^+]_i}{dt} = J_{\text{Na/K},i} - J_{\text{KIR},i} - J_{\text{K},i} \quad (39)$$

$\gamma_i$	Change in membrane potential by a scaling factor	$1970 \text{ mV}\mu\text{M}^{-1}$	[7]
$\lambda_i$	Rate constant for opening	$45.0 \text{ s}^{-1}$	[7]

## Endothelial cell

Cytosolic  $\text{Ca}^{2+}$  concentration in the EC (in  $\mu\text{M}$ ):

$$\begin{aligned} \frac{d[\text{Ca}^{2+}]_j}{dt} = & J_{\text{IP}_3,j} - J_{\text{upt},j} + J_{\text{CICR}_j} - J_{\text{extr},j} \dots \\ & + J_{\text{leak},j} + J_{\text{cation}_j} + J_{0_j} + J_{\text{stretch},j} - J_{\text{Ca}^{2+}\text{-coupling}_j}^{\text{SMC-EC}} \end{aligned} \quad (40)$$

$\text{Ca}^{2+}$  concentration in the ER in the EC (in  $\mu\text{M}$ ):

$$\frac{d[\widehat{\text{Ca}^{2+}}]_j}{dt} = J_{\text{upt},j} - J_{\text{CICR}_j} - J_{\text{leak},j} \quad (41)$$

Membrane potential of the EC (in mV):

$$\frac{dv_j}{dt} = -\frac{1}{C_{m_j}} (J_{K_j} + J_{R_j}) + V_{\text{coupling}_j}^{\text{SMC-EC}} \quad (42)$$

$\text{IP}_3$  concentration of the EC (in  $\mu\text{M}$ ):

$$\frac{d[\text{IP}_3]_j}{dt} = J_{\text{EC,IP}_3} - J_{\text{degr},j} - J_{\text{IP}_3\text{-coupling}_j}^{\text{SMC-EC}} \quad (43)$$

$C_{m_j}$	Membrane capacitance	25.8 pF	[7]
$J_{PLC}$	PLC / $IP_3$ production rate	0.18 or 0.4 $\mu M s^{-1}$	[7]
$J_{0_j}$	Constant $Ca^{2+}$ leak term (influx)	0.029 $\mu M s^{-1}$	[7]

## Fluxes

### Smooth muscle cell

Release of calcium from  $IP_3$  sensitive stores in the SMC (in  $\mu M s^{-1}$ ):

$$J_{IP_3,i} = F_i \frac{[IP_3]_i^2}{K_{ri}^2 + [IP_3]_i^2} \quad (44)$$

$F_i$	Maximal rate of activation-dependent calcium influx	0.23 $\mu M s^{-1}$	[7]
$K_{ri}$	Half-saturation constant for agonist-dependent calcium entry	1 $\mu M$	[7]

Uptake of calcium into the sarcoplasmic reticulum (in  $\mu M s^{-1}$ ):

$$J_{upt,i} = B_i \frac{[Ca^{2+}]_i^2}{c_{bi}^2 + [Ca^{2+}]_i^2} \quad (45)$$

$B_i$	SR uptake rate constant	2.025 $\mu M s^{-1}$	[7]
$c_{bi}$	Half-point of the SR ATPase activation sigmoidal	1.0 $\mu M$	[7]

Calcium-induced calcium release (CICR; in  $\mu M s^{-1}$ ):

$$J_{CICR_i} = C_i \frac{[\widehat{Ca^{2+}}]_i^2}{s_{ci}^2 + [\widehat{Ca^{2+}}]_i^2} \frac{[Ca^{2+}]_i^4}{c_{ci}^4 + [Ca^{2+}]_i^4} \quad (46)$$

$C_i$	CICR rate constant	55 $\mu M s^{-1}$	[7]
$s_{ci}$	Half-point of the CICR $Ca^{2+}$ efflux sigmoidal	2.0 $\mu M$	[7]
$c_{ci}$	Half-point of the CICR activation sigmoidal	0.9 $\mu M$	[7]

Calcium extrusion by  $Ca^{2+}$ -ATPase pumps (in  $\mu M s^{-1}$ ):

$$J_{extr,i} = D_i [Ca^{2+}]_i \left( 1 + \frac{v_i - v_d}{R_{di}} \right) \quad (47)$$

$D_i$	Rate constant for $\text{Ca}^{2+}$ extrusion by the ATPase pump	$0.24 \text{ s}^{-1}$	[7]
$v_d$	Intercept of voltage dependence of extrusion ATPase	-100.0 mV	[7]
$R_{di}$	Slope of voltage dependence of extrusion ATPase.	250.0 mV	[7]
<hr/>			
$L_i$	Leak from SR rate constant	$0.025 \text{ s}^{-1}$	[7]

Leak current from the SR (in  $\mu\text{M s}^{-1}$ ):

$$J_{\text{leak},i} = L_i[\widehat{\text{Ca}^{2+}}]_i \quad (48)$$

Calcium influx through VOCCs (in  $\mu\text{M s}^{-1}$ ):

$$J_{\text{VOCC},i} = G_{\text{Ca},i} \frac{v_i - v_{\text{Ca1},i}}{1 + \exp(-[(v_i - v_{\text{Ca2},i}) / R_{\text{Ca},i}])} \quad (49)$$

$G_{\text{Ca},i}$	Whole-cell conductance for VOCCs	$1.29 \times 10^{-3} \mu\text{M mV}^{-1} \text{s}^{-1}$	[7]
$v_{\text{Ca1},i}$	Reversal potential for VOCCs	100.0 mV	[7]
$v_{\text{Ca2},i}$	Half-point of the VOCC activation sigmoidal	-24.0 mV	[7]
$R_{\text{Ca},i}$	Maximum slope of the VOCC activation sigmoidal	8.5 mV	[7]

Flux of calcium exchanging with sodium in the  $\text{Na}^+\text{Ca}^{2+}$  exchange (in  $\mu\text{M s}^{-1}$ ):

$$J_{\text{Na/Ca},i} = G_{\text{Na/Ca},i} \frac{[\text{Ca}^{2+}]_i}{[\text{Ca}^{2+}]_i + c_{\text{Na/Ca},i}} (v_i - v_{\text{Na/Ca},i}) \quad (50)$$

$G_{\text{Na/Ca},i}$	Whole-cell conductance for $\text{Na}^+/\text{Ca}^{2+}$ exchange	$3.16 \times 10^{-3} \mu\text{M mV}^{-1}\text{s}^{-1}$	[7]
$c_{\text{Na/Ca},i}$	Half-point for activation of $\text{Na}^+/\text{Ca}^{2+}$ exchange by $\text{Ca}^{2+}$	0.5 $\mu\text{M}$	[7]
$v_{\text{Na/Ca},i}$	Reversal potential for the $\text{Na}^+/\text{Ca}^{2+}$ exchanger	-30.0 mV	[7]

Calcium flux through the stretch-activated channels in the SMC (in  $\mu\text{M s}^{-1}$ ):

$$J_{\text{stretch},i} = \frac{G_{\text{stretch}}}{1 + \exp\left(-\alpha_{\text{stretch}}\left(\frac{\Delta p R}{h} - \sigma_0\right)\right)} (v_i - E_{\text{SAC}}) \quad (51)$$

$G_{\text{stretch}}$	Whole cell conductance for SACs	$6.1 \times 10^{-3} \mu\text{M mV}^{-1}\text{s}^{-1}$	[7]
$\alpha_{\text{stretch}}$	Slope of stress dependence of the SAC activation sigmoidal	$7.4 \times 10^{-3} \text{ mmHg}^{-1}$	[7]
$\Delta p$	Pressure difference	30 mmHg	ME
$\sigma_0$	Half-point of the SAC activation sigmoidal	500 mmHg	[7]
$E_{\text{SAC}}$	Reversal potential for SACs	-18 mV	[7]

Flux through the sodium potassium pump (in  $\mu\text{M s}^{-1}$ ):

$$J_{\text{Na/K},i} = F_{\text{Na/K},i} \quad (52)$$

$F_{\text{Na/K},i}$	Rate of the potassium influx by the sodium potassium pump	$4.32 \times 10^{-2} \mu\text{M s}^{-1}$	[7]
---------------------	---	--	-----

Chloride flux through the chloride channel (in  $\mu\text{M s}^{-1}$ ):

$$J_{\text{Cl},i} = G_{\text{Cl},i} (v_i - v_{\text{Cl},i}) \quad (53)$$

$G_{\text{Cl},i}$	Whole-cell conductance for $\text{Cl}^-$ current	$1.34 \times 10^{-3} \mu\text{M mV}^{-1}\text{s}^{-1}$	[7]
$v_{\text{Cl},i}$	Reversal potential for $\text{Cl}^-$ channels.	-25.0 mV	[7]

Potassium flux through potassium channel (in  $\mu\text{M s}^{-1}$ ):

$$J_{\text{K},i} = G_{\text{K},i} w_i (v_i - v_{\text{K},i}) \quad (54)$$

$G_{K,i}$	Whole-cell conductance for $K^+$ efflux.	$4.46 \times 10^{-3} \mu M mV^{-1} s^{-1}$	[7]
$v_{K,i}$	Nernst potential	-94 mV	[7]
$F_{KIR,i}$	Scaling factor of potassium efflux through the KIR channel	750 mV $\mu M^{-1}$	[4]

Flux through KIR channels in the SMC (in  $\mu M s^{-1}$ ):

$$J_{KIR,i} = \frac{F_{KIR,i} g_{KIR,i}}{\gamma_i} (v_i - v_{KIR,i}) \quad (55)$$

IP<sub>3</sub> degradation (in  $\mu M s^{-1}$ ):

$$J_{degr,i} = k_{d,i} [IP_3]_i \quad (56)$$

$k_{d,i}$	Rate constant of IP <sub>3</sub> degradation	0.1 $s^{-1}$	[7]
-----------	--	--------------	-----

## Endothelial cell

Release of calcium from IP<sub>3</sub>-sensitive stores in the EC (in  $\mu M s^{-1}$ ):

$$J_{IP_3,j} = F_j \frac{[IP_3]_j^2}{K_{rj}^2 + [IP_3]_j^2} \quad (57)$$

$F_j$	Maximal rate of activation-dependent calcium influx	0.23 $\mu M s^{-1}$	[7]
$K_{rj}$	Half-saturation constant for agonist-dependent calcium entry	1 $\mu M$	[7]

Uptake of calcium into the endoplasmic reticulum (in  $\mu M s^{-1}$ ):

$$J_{upt,j} = B_j \frac{[Ca^{2+}]_j^2}{c_{bj}^2 + [Ca^{2+}]_j^2} \quad (58)$$

$B_j$	ER uptake rate constant	0.5 $\mu M s^{-1}$	[7]
$c_{bj}$	Half-point of the SR ATPase activation sigmoidal	1.0 $\mu M$	[7]

Calcium-induced calcium release (CICR; in  $\mu M s^{-1}$ ):

$$J_{CICR_j} = C_j \frac{[\widehat{Ca^{2+}}]_j^2}{s_{cj}^2 + [\widehat{Ca^{2+}}]_j^2} \frac{[Ca^{2+}]_j^4}{c_{cj}^4 + [Ca^{2+}]_j^4} \quad (59)$$

$C_j$	CICR rate constant	$5 \mu\text{M s}^{-1}$	[7]
$s_{cj}$	Half-point of the CICR $\text{Ca}^{2+}$ efflux sigmoidal	$2.0 \mu\text{M}$	[7]
$c_{cj}$	Half-point of the CICR activation sigmoidal	$0.9 \mu\text{M}$	[7]

Calcium extrusion by  $\text{Ca}^{2+}$ -ATPase pumps (in  $\mu\text{M s}^{-1}$ ):

$$J_{\text{extr},j} = D_j[\text{Ca}^{2+}]_j \quad (60)$$

$D_j$	Rate constant for $\text{Ca}^{2+}$ extrusion by the ATPase pump	$0.24 \text{ s}^{-1}$	[8]
-------	---	-----------------------	-----

Calcium flux through the stretch-activated channels in the EC (in  $\mu\text{M s}^{-1}$ ):

$$J_{\text{stretch},j} = \frac{G_{\text{stretch}}}{1 + e^{-\alpha_{\text{stretch}}(\sigma - \sigma_0)}} (v_j - E_{\text{SAC}}) = \frac{G_{\text{stretch}}}{1 + e^{-\alpha_{\text{stretch}}(\frac{\Delta p R}{h} - \sigma_0)}} (v_j - E_{\text{SAC}}) \quad (61)$$

$G_{\text{stretch}}$	The whole cell conductance for SACs	$6.1 \times 10^{-3} \mu\text{M mV}^{-1} \text{s}^{-1}$	[7]
$\alpha_{\text{stretch}}$	Slope of stress dependence of the SAC activation sigmoidal	$7.4 \times 10^{-3} \text{ mmHg}^{-1}$	[7]
$\Delta p$	Pressure difference	$30 \text{ mmHg}$	ME
$\sigma_0$	Half-point of the SAC activation sigmoidal	$500 \text{ mmHg}$	[7]
$E_{\text{SAC}}$	The reversal potential for SACs	$-18 \text{ mV}$	[7]

Leak current from the ER (in  $\mu\text{M s}^{-1}$ ):

$$J_{\text{leak},j} = L_j[\widehat{\text{Ca}^{2+}}]_j \quad (62)$$

$L_j$	Rate constant for $\text{Ca}^{2+}$ leak from the ER	$0.025 \text{ s}^{-1}$	[7]
-------	---	------------------------	-----

Calcium influx through nonselective cation channels (in  $\mu\text{M s}^{-1}$ ):

$$J_{\text{cation}_j} = G_{\text{cat}_j}(E_{\text{Ca}_j} - v_j) \frac{1}{2} \left( 1 + \tanh \left( \frac{\log_{10}[\text{Ca}^{2+}]_j - m_{3\text{cat}_j}}{m_{4\text{cat}_j}} \right) \right) \quad (63)$$

Potassium efflux through the  $J_{BK_{Ca_j}}$  channel and the  $J_{SK_{Ca_j}}$  channel (in  $\mu\text{M s}^{-1}$ ):

$$J_{K_j} = G_{\text{tot}_j}(v_j - v_{K_j}) (J_{BK_{Ca_j}} + J_{SK_{Ca_j}}) \quad (64)$$

table  
ist  
dop-  
pelt?!

$G_{catj}$	Whole-cell cation channel conductivity	$6.6 \times 10^{-4} \mu\text{M mV}^{-1}\text{s}^{-1}$	[7]
$E_{Ca j}$	$\text{Ca}^{2+}$ equilibrium potential	50 mV	[7]
$m_{3catj}$	Model constant	-0.18 $\mu\text{M}$	[7]
$m_{4catj}$	Model constant	0.37 $\mu\text{M}$	[7]

---

$G_{totj}$	Total potassium channel conductivity.	6927 pS	[7]
$v_{Kj}$	$\text{K}^+$ equilibrium potential	-80.0 mV	[7]

Potassium efflux through the  $J_{BK_{Ca j}}$  channel (in  $\mu\text{M s}^{-1}$ ):

$$J_{BK_{Ca j}} = 0.2 \left( 1 + \tanh \left( \frac{(\log_{10}[\text{Ca}^{2+}]_j - c)(v_j - b_j) - a_{1j}}{m_{3bj}(v_j + a_{2j}(\log_{10}[\text{Ca}^{2+}]_j - c) - b_j)^2 + m_{4bj}} \right) \right) \quad (65)$$

Potassium efflux through the  $J_{SK_{Ca j}}$  channel (in  $\mu\text{M s}^{-1}$ ):

$$J_{SK_{Ca j}} = 0.3 \left( 1 + \tanh \left( \frac{\log_{10}[\text{Ca}^{2+}]_j - m_{3sj}}{m_{4sj}} \right) \right) \quad (66)$$

$c$	Model constant, further explanation see reference	-0.4 $\mu\text{M}$	[7]
$b_j$	Model constant, further explanation see reference	-80.8 mV	[7]
$a_{1j}$	Model constant, further explanation see reference	53.3 $\mu\text{M mV}$	[7]
$a_{2j}$	Model constant, further explanation see reference	53.3 mV $\mu\text{M}^{-1}$	[7]
$m_{3bj}$	Model constant, further explanation see reference	$1.32 \times 10^{-3} \mu\text{M mV}^{-1}$	[7]
$m_{4bj}$	Model constant, further explanation see reference	0.30 $\mu\text{M mV}$	[7]
$m_{3sj}$	Model constant, further explanation see reference	-0.28 $\mu\text{M}$	[7]
$m_{4sj}$	Model constant, further explanation see reference	0.389 $\mu\text{M}$	[7]

Residual current regrouping chloride and sodium current flux (in  $\mu\text{M s}^{-1}$ ):

$$J_{R_j} = G_{R_j}(v_j - v_{\text{rest},j}) \quad (67)$$

$G_{R_j}$	Residual current conductivity	955 pS	[7]
$v_{\text{rest},j}$	Membrane resting potential	-31.1 mV	[7]

$\text{IP}_3$  degradation (in  $\mu\text{M s}^{-1}$ ):

$$J_{\text{degr},j} = k_{d,j}[\text{IP}_3]_j \quad (68)$$

$k_{d,j}$	Rate constant of IP <sub>3</sub> degradation	$0.1 \text{ s}^{-1}$	[7]
-----------	--	----------------------	-----

## Coupling

Heterocellular electrical coupling between SMCs and ECs (in mV s<sup>-1</sup>):

$$V_{coupling_i}^{SMC-EC} = -G_{coup}(v_i - v_j) \quad (69)$$

Heterocellular IP<sub>3</sub> coupling between SMCs and ECs (in μM s<sup>-1</sup>):

$$J_{IP_3-coupling_i}^{SMC-EC} = -P_{IP_3}([IP_3]_i - [IP_3]_j) \quad (70)$$

Calcium coupling with EC (in μM s<sup>-1</sup>):

$$J_{Ca^{2+}-coupling_i}^{SMC-EC} = -P_{Ca^{2+}}([Ca^{2+}]_i - [Ca^{2+}]_j) \quad (71)$$

$G_{coup}$	Heterocellular electrical coupling coefficient	$0.5 \text{ s}^{-1}$	ME
$P_{IP_3}$	Heterocellular IP <sub>3</sub> coupling coefficient	$0.05 \text{ s}^{-1}$	[7]
$P_{Ca^{2+}}$	Heterocellular $P_{Ca^{2+}}$ coupling coefficient	$0.05 \text{ s}^{-1}$	[7]

## Additional Equations

Equilibrium distribution of open channel states for the voltage and calcium activated potassium channels (dimensionless):

$$K_{act_i} = \frac{([Ca^{2+}]_i + c_{wi})^2}{([Ca^{2+}]_i + c_{wi})^2 + \beta_i \exp(-([v_i - v_{Ca_{3i}}]/R_{Ki}))} \quad (72)$$

Nernst potential of the KIR channel in the SMC (in mV):

$$v_{KIR,i} = z_1[K^+]_p - z_2 \quad (73)$$

Conductance of KIR channel (in μM mV<sup>-1</sup> s<sup>-1</sup>):

$$g_{KIR,i} = \exp(z_5 v_i + z_3[K^+]_p - z_4) \quad (74)$$



$c_{wi}$	Translation factor for $\text{Ca}^{2+}$ dependence of $\text{K}_{Ca}$ channel activation sigmoidal.	0.0 $\mu\text{M}$	[7]
$\beta_i$	Translation factor for membrane potential dependence of $\text{K}_{Ca}$ channel activation sigmoidal.	0.13 $\mu\text{M}^2$	[7]
$v_{Ca_{3i}}$	Half-point for the $\text{K}_{Ca}$ channel activation sigmoidal.	-27 mV	[7]
$R_{Ki}$	Maximum slope of the $\text{K}_{Ca}$ activation sigmoidal.	12 mV	[7]
$z_1$	Model estimation for membrane voltage KIR channel	$4.5 \times 10^3 \text{ mV} \mu\text{M}^{-1}$	[3]
$z_2$	Model estimation for membrane voltage KIR channel	112 mV	[3]
$z_3$	Model estimation for the KIR channel conductance	$4.2 \times 10^2 \text{ mV}^{-1} \text{s}^{-1}$	[3]
$z_4$	Model estimation for the KIR channel conductance	$12.6 \mu\text{M mV}^{-1} \text{s}^{-1}$	[3]
$z_5$	Model estimation for the KIR channel conductance	$-7.4 \times 10^{-2} \mu\text{M mV}^{-2} \text{s}^{-1}$	[3]

### 6.3 The Contraction Model

Fraction of free phosphorylated cross-bridges (dimensionless):

$$\frac{d[MP]}{dt} = K_4[AMP] + K_1[M] - (K_2 + K_3)[MP] \quad (75)$$

Fraction of attached phosphorylated cross-bridges (dimensionless):

$$\frac{d[AMP]}{dt} = K_3[MP] + K_6[AM] - (K_4 + K_5)[AMP] \quad (76)$$

Fraction of attached dephosphorylated cross-bridges (dimensionless):

$$\frac{d[AM]}{dt} = K_5[AMP] - (K_7 + K_6)[AM] \quad (77)$$

Fraction of free non-phosphorylated cross-bridges (dimensionless):

$$[M] = 1 - [AM] - [AMP] - [MP] \quad (78)$$

Rate constants that represent phosphorylation of M to Mp and of AM to AMp by the active myosin light chain kinase (MLCK), respectively (in  $\text{s}^{-1}$ ):

$$K_1 = K_6 = \gamma_{cross} [\text{Ca}^{2+}]_i^{n_{cross}} \quad (79)$$

### 6.4 The Mechanical Model

Wall thickness of the vessel (in  $\mu\text{m}$ ):

$$h = 0.1R \quad (80)$$

Fraction of attached myosin cross-bridges (dimensionless):

$$F_r = [AMP] + [AM] \quad (81)$$

$K_2$	Rate constant for dephosphorylation (of Mp to M) by myosin light-chain phosphatase (MLCP)	$0.5 \text{ s}^{-1}$	[6]
$K_3$	Rate constants representing the attachment/detachment of fast cycling phosphorylated crossbridges	$0.4 \text{ s}^{-1}$	[6]
$K_4$	Rate constants representing the attachment/detachment of fast cycling phosphorylated crossbridges	$0.1 \text{ s}^{-1}$	[6]
$K_5$	Rate constant for dephosphorylation (of AMp to AM) by myosin light-chain phosphatase (MLCP)	$0.5 \text{ s}^{-1}$	[6]
$K_7$	Rate constant for latch-bridge detachment	$0.1 \text{ s}^{-1}$	[6]
$\gamma_{cross}$	Sensitivity of the contractile apparatus to calcium	$17 \text{ }\mu\text{M}^{-3} \text{ s}^{-1}$	[8]
$n_{cross}$	Fraction constant of the phosphorylation crossbridge	3 [-]	[8]

Vessel radius (in m):

$$\frac{dR}{dt} = \frac{R_{0_{pas}}}{\eta} \left( \frac{RP_T}{h} - E(F_r) \frac{R - R_0(F_r)}{R_0(F_r)} \right) \quad (82)$$

with:

$$E(F_r) = E_{pas} + F_r (E_{act} - E_{pas}) \quad (83)$$

$$R_0(F_r) = R_{0_{pas}} + F_r (\alpha_r - 1) R_{0_{pas}} \quad (84)$$

$\eta$	viscosity	$10^4$ Pa s	[7]
$R_{0_{pas}}$	Radius of the vessel when passive and no stress is applied	20 $\mu\text{m}$	ME
$P_T$	Transmural pressure	$4 \times 10^3$ Pa	ME
$E_{pas}$	Young's modulus for the passive vessel	$66 \times 10^3$ Pa	[5]
$E_{act}$	Young's modulus for the active vessel	$233 \times 10^3$ Pa	[5]
$\alpha_r$	Scaling factor initial radius	0.6	[5]

## References

- [1] **Donk, L. V. D. and Kock, E. G. J. D. (2013):** Bluefern Supercomputing Unit University of Canterbury Eindhoven University of Technology.
- [2] **Filosa, J. A.; Bonev, A. D. and Nelson, M. T. (2004):** Calcium dynamics in cortical astrocytes and arterioles during neurovascular coupling., *Circulation research*, Vol. 95, No. 10 pp. e73–81.
- [3] **Filosa, J. a.; Bonev, A. D.; Straub, S. V.; Meredith, A. L.; Wilkerson, M. K.; Aldrich, R. W. and Nelson, M. T. (2006):** Local potassium signaling couples neuronal activity to vasodilation in the brain., *Nature neuroscience*, Vol. 9, No. 11 pp. 1397–1403.
- [4] **Gonzalez-fernandez, J. M. and Ermentrout, B. (1994):** On the origin and dynamics of the vasomotion of small arteries, *Mathematical biosciences*, Vol. 119, No. 2 pp. 127–167.
- [5] **Gore, R. W. and Davis, M. J. (1985):** Mechanics of Smooth Muscle in Isolated Single Microvessels, Vol. 12 pp. 511–520.
- [6] **Hai, C.-m. and Murphy, R. A. (1989):** Ca<sup>2+</sup> Crossbridge Phosphorylation, and Contraction, *Annual review of physiology*, Vol. 51, No. 1 pp. 285–298.
- [7] **Koenigsberger, M.; Sauser, R.; Bény, J.-L. J. and Meister, J. J.-J. (2006):** Effects of arterial wall stress on vasomotion, *Biophysical journal*, Vol. 91, No. September pp. 1663–1674.
- [8] **Koenigsberger, M.; Sauser, R.; Bény, J.-L. L.; Meister, J.-J. J. and Be, J.-l. (2005):** Role of the endothelium on arterial vasomotion, *Biophysical journal*, Vol. 88, No. 6 pp. 3845–3854.
- [9] **Nagelhus, E.; Horio, Y. and Inanobe, A. (1999):** Immunogold evidence suggests that coupling of K<sup>+</sup> siphoning and water transport in rat retinal muller cells is mediated by a coenrichment of kir4. 1 and aqp4 in specific membrane domains, *Glia*, Vol. 63, No. 1 pp. 47–54.
- [10] **Ø stby, I.; Ø yehaug, L.; Einevoll, G. T.; Nagelhus, E. A.; Plahte, E.; Zeuthen, T.; Lloyd, C. M.; Ottersen, O. P. and Omholt, S. W. (2009):** Astrocytic Mechanisms Explaining Neural-Activity-Induced Shrinkage of Extraneuronal Space, *PLoS Computational Biology*, Vol. 5, No. 1 pp. 1–12.
- [11] **Shipp, S. (2007):** Structure and function of the cerebral cortex., *Current biology : CB*, Vol. 17, No. 12 pp. R443—9.

